Theory of carrier motion in dynamically disordered systems

Roger F. Loring, Massimo Sparpaglione, and Shaul Mukamel[a)]
Department of Chemistry, University of Rochester, Rochester, New York 14627

(Received 4 September 1986; accepted 28 October 1986)

We present a quantum mechanical theory of the dynamics of a charge carrier or an electronic excitation in a condensed phase system, in which the solvent degrees of freedom that couple to the electronic excitation are characterized by a correlation time of arbitrary magnitude. We consider a charge carrier moving among active sites that are randomly distributed in space. The site energies undergo stochastic modulation with a finite correlation time, through the interactions with the solvent. A mode-coupling self-consistent equation is derived from which transport properties such as the ac conductivity, the mean-squared displacement, and the time-dependent probability that a carrier remains on the initial site are calculated. A metal–insulator transition is predicted in three dimensions, but not in one or two dimensions, in agreement with the scaling theory of Anderson localization. The present treatment allows the investigation of carrier dynamics even when there is no separation of time scales between the dynamics of carrier and solvent.

I. INTRODUCTION

The interaction of an electronic excitation or a charge carrier with the nuclear degrees of freedom of the surrounding medium is a central topic in the chemistry and physics of condensed phases. Such interactions play a crucial role in the dynamics of excess electrons in solution[1–4] and in the electrical conductivity of disordered materials such as solid electrolytes.[5,6] The problem of carrier motion in a condensed phase medium is considerably simplified, when the correlation time of the medium (hereafter denoted "the solvent") is short compared to the time scale of the carrier dynamics. In this case, it is possible to construct an effective Liouville operator for the carrier, in which the effect of the solvent is given by a dephasing rate or friction. The Haken–Strobl model[7] of exciton motion in molecular crystals, in which the phonons enter through a dephasing rate, is based on such a separation of time scales. An analogous issue arises in the theory of chemical reactions in solution. The treatment of chemical kinetics in solution is simplified when there is a separation of time scales between the solvent dynamics and the motion of the reactive system along the reaction coordinate. The Kramers model of activated barrier crossing in solution, in which the effect of the solvent is represented by a constant (frequency independent) friction, is based on this separation of time scales.[8] Experimental measurements of photoisomerization rates in solution for some systems show deviations from the predictions of Kramers theory.[9] These discrepancies were treated in the theories of Grote and Hynes[10] and Bagchi and Oxtoby,[11] in which the friction is given a frequency dependence, which reflects the finite time scale of the solvent dynamics. The dynamics of electronic excitations interacting with nuclear degrees of freedom whose time scale is not necessarily short compared to the time scale of the excitation have received considerable attention from theorists.[12–19] Chandler and co-workers have applied path integral methods to the investigation of the solvation of excess electrons in a fluid.[20] Sumi has investigated a model of exciton dynamics in molecular crystals, in which the system is represented by an ordered lattice with site energies that are Gaussian, stochastic variables, whose fluctuations are characterized by a finite time scale (colored noise).[12] He calculated the absorption line shape within the coherent potential approximation (CPA). Blumen and Silbey have obtained similar results for the absorption line shape for this model with a truncated cumulant expansion.[13] It should be emphasized that the absorption line shape does not contain sufficient information to yield transport properties, such as the mean-squared-displacement of an excitation. In general, the approximate methods that are used to calculate a line shape or density of states cannot be extended in a simple way to the calculation of transport properties, and new methods must be developed. An example is the two-particle CPA of Velicky[21–23] which, however, does not have the capacity to predict a metal–insulator transition. Recently, Druger, Ratner, and Nitzan,[6] and Harrison and Zwanzig[24] have considered models of transport in disordered media based on a Pauli master equation, in which the rates at which the excitation hops from site to site are time-dependent random variables. Harrison and Zwanzig[24] considered a model in which the rates between different pairs of sites fluctuate independently, and calculated transport properties within the effective medium approximation. Similar results were obtained by Druger, Ratner, and Nitzan[6] who performed an exact calculation for a model in which the entire disordered lattice is randomly renewed at a constant rate.

In this work, we present a theory of carrier dynamics in a condensed phase system that is characterized both by static and dynamic sources of disorder. We consider a model in which noninteracting carriers move among active sites that are randomly distributed on a lattice, with site energies that are stochastic variables whose fluctuations are characterized by a time scale of arbitrary magnitude. The model treated here unifies a variety of models that have been extensively studied in condensed matter physics. The model is characterized by three parameters: c the concentration of active sites, Δ the root-mean-squared magnitude of the site energy fluctuations, and Λ the inverse correlation time of the fluctuations. We consider six limiting cases. First, for $c = 1$ (or-

[a)] Camille and Henry Dreyfus Teacher–Scholar.

 0021-9606/87/042249-15$02.10

dered lattice), $\Delta > 0$, and $\Lambda > 0$, we recover the model of excitons in molecular crystals that was treated by Sumi,[12] and by Blumen and Silbey.[13] Second, for $c = 1$ and $\Delta = 0$ (no energetic disorder), the model describes a perfect lattice of interacting, quantum mechanical, two-level systems.[25] Third, for $c = 1$ and $\Lambda = 0$ (static energy disorder), the model reduces to the much studied Anderson model, which displays a metal/insulator phase transition (Anderson localization).[26–33] Fourth, for $\Delta = 0$ and $c < 1$, the model reduces to the quantum percolation problem, which has been the subject of several recent studies.[33–36] Fifth, for $c = 1$ and $\Lambda \gg \Delta$, there is a separation of time scales between the energy fluctuations and the carrier motion, and the Haken–Strobl model of exciton dynamics in molecular crystals is recovered.[7] Sixth, for $\Lambda \gg \Delta$ and $\Delta^2/\Lambda \gg J$, the Liouville equation reduces to a Pauli master equation with a site-to-site hopping rate of $J^2\Lambda/\Delta^2$. This limit describes incoherent exciton motion.[37–39] Logan and Wolynes (LW) have investigated the metal–insulator transition for a model that includes static, energetic disorder and topological disorder.[40] Within the present model, this corresponds to $\Lambda = 0$, $\Delta > 0$, and $c < 1$. LW incorporated the pair correlation function of the fluid in their treatment, and calculated the density of states, using an extension to topological disorder of the self-consistent method of Abou-Chacra, Anderson, and Thouless.[27] A calculation of the density of states cannot be simply extended to determine the transport properties that we calculate here, such as the ac conductivity.

The present model corresponds to a quantum mechanical treatment of the carrier, and a classical treatment of the solvent degrees of freedom with which the carrier interacts. It should be noted that in such a stochastic treatment, the action of the carrier on the surrounding medium is neglected; that is, the "bath" affects the "system," but the "system" does not affect the "bath". In other words, polaron effects[18] are not included in this stochastic approach. The present theory is the first quantum theory of carrier transport in a medium that is characterized by static disorder and by dynamic disorder with an arbitrary time scale.

In Sec. II, we use linear response theory to derive the exact relation between the ac electrical conductivity and the density–density correlation function of the charge carriers. We then outline the approximations by which the ac conductivity can be related to the frequency dependent diffusion kernel. This latter result will be used in our theory of the ac conductivity. In Sec. III, we present the model, and derive a self-consistent mode-coupling equation from which transport properties are calculated, such as the ac conductivity, the mean-squared-displacement, and the time-dependent probability that a carrier remains on the initial site. This derivation represents an extension to a model with dynamical disorder of an approach that has been applied to several related models with static disorder: quantum percolation,[41] Anderson localization,[42] and a model of transport in disordered media that is based on a Pauli master equation.[39] The behavior of transport properties at long times and small frequencies is determined analytically in Sec. IV. A metal–insulator transition is predicted to occur in three dimensions. Below a critical value of the concentration of active sites, carriers are confined to a finite volume, while above this concentration, carriers can explore the entire system. If the correlation time of the solvent is finite, this critical concentration is independent of the magnitude of the energetic disorder. This result is intuitively reasonable, since for time scales long compared to the solvent correlation time, the carrier moves in a dynamically averaged potential. If the correlation time is infinite and the solvent creates a *static* random potential for the carrier, then the critical concentration depends on the width of the distribution of site energies. No transition is predicted in one or two dimensions, in accordance with the scaling theory of Anderson localization.[43,44] Numerical calculations of transport properties for a wide range of times and frequencies are presented and discussed in Sec. V. If the motion of the medium is slow compared to the time associated with the motion of the carrier from one site to another, the carrier can be localized in a finite volume for times small compared to the correlation time of the medium, but will eventually explore the entire system at longer times. This result emphasizes that a formal, asymptotic, long-time analysis may be misleading, since the times required to attain such a limit may be extremely long compared to experimentally relevant times. A material that has a nonzero dc conductivity (a conductor) may still behave like an insulator over a wide range of frequencies, as is shown by the detailed calculations presented in Sec. V. Our work is summarized in Sec. VI.

II. FORMAL RELATION OF THE ELECTRICAL CONDUCTIVITY TO THE DENSITY–DENSITY CORRELATION FUNCTION AND THE DENSITY PROPAGATOR

We consider a fluid of N particles in a volume Ω, governed by the Hamiltonian

$$\tilde{H} = H - (1/2)\sum_{m=1}^{N} [A_m F(\mathbf{r}_m,t) + F(\mathbf{r}_m,t)A_m]. \tag{2.1}$$

H is the system Hamiltonian in the absence of the external field, and the second term represents the interaction of system and field. $F(\mathbf{r},t)$ is the external field which is coupled to the particle labeled m at position $\mathbf{r}_m$ through the operator A_m, which is a single-body operator depending only on the degrees of freedom of particle m. In linear response theory, the expectation value of a system observable B is expressed as an equilibrium response function, which can be calculated from a knowledge of the dynamics of the system in the absence of the external field.[45–49] In this section, we establish general, formal relationships between four dynamical quantities that are associated with the linear response of a system to an external perturbation: the response function, Φ_{BA}, the Kubo transform of the response function, $\hat{\Phi}_{BA}$, the correlation function, $\mathscr{C}_{BA}$, and the propagator, $\mathscr{G}_{BA}$. The electrical conductivity is conventionally written in terms of the density response function $\Phi_{\rho\rho}$. The density of charge carriers is denoted ρ. However, it is more convenient to develop a microscopic theory for the density propagator $\mathscr{G}_{\rho\rho}$. We use the relations outlined in this section to establish a rigorous connection between $\Phi_{\rho\rho}$ and $\mathscr{C}_{\rho\rho}$. We then derive an approximate relation between $\mathscr{C}_{\rho\rho}$ and $\mathscr{G}_{\rho\rho}$. In Secs. III–V, we shall

use this relation to determine the conductivity from a self-consistent calculation of $\mathscr{G}_{\rho\rho}$.

Expanding $F(\mathbf{r},t)$ in the spatial Fourier series

$$F(\mathbf{r}_m,t) = N^{-1}\sum_{\mathbf{q}} \exp(-i\mathbf{q}\cdot\mathbf{r}_m)F_{\mathbf{q}}(t) \tag{2.2}$$

and substituting this expansion into Eq. (2.1) yields

$$\tilde{H} = H - N^{-1}\sum_{\mathbf{q}} A_{-\mathbf{q}}F_{\mathbf{q}}(t). \tag{2.3}$$

The spatial Fourier transform of A_m is defined by

$$A_{\mathbf{q}} = \sum_m [A_m \exp(i\mathbf{q}\cdot\mathbf{r}_m) + \exp(i\mathbf{q}\cdot\mathbf{r}_m)A_m]. \tag{2.4}$$

Since we are treating the linear response of the system to the field F, we need only consider a single Fourier component of the Hamiltonian in Eq. (2.3). The expectation value of an operator $B_{\mathbf{q}}$ at time t is given by

$$\langle B_{\mathbf{q}}(t)\rangle = \int_0^t d\tau\, \Phi_{BA}(\mathbf{q},t-\tau)F_{\mathbf{q}}(\tau). \tag{2.5}$$

Φ is the *response function*, defined by

$$\Phi_{BA}(\mathbf{q},t) = (i/\hbar)\mathrm{Tr}\{[B_{\mathbf{q}}(t), A_{-\mathbf{q}}]\hat{\rho}_{\mathrm{eq}}\}, \tag{2.6a}$$

$$B_{\mathbf{q}}(t) = \exp[(iH/\hbar)t]B_{\mathbf{q}}\exp[-iH/\hbar)t], \tag{2.6b}$$

$$\hat{\rho}_{\mathrm{eq}} = \exp(-\beta H)/\mathrm{Tr}\{\exp(-\beta H)\}. \tag{2.6c}$$

$\hat{\rho}_{\mathrm{eq}}$ is the canonical equilibrium density matrix, and $\beta = 1/kT$. In the remainder of this work, the density matrix will be denoted $\hat{\rho}$ to avoid confusion with ρ, the charge carrier density. It is useful to define three other quantities that are associated with the system response to an external perturbation. The *Kubo transform* of the response function is defined by

$$\hat{\Phi}_{BA}(\mathbf{q},t) = \int_0^\beta d\lambda\, \mathrm{Tr}\{\exp(\lambda H)A_{-\mathbf{q}} \times \exp(-\lambda H)B_{\mathbf{q}}(t)\hat{\rho}_{\mathrm{eq}}\}, \tag{2.7}$$

the *correlation function* of operators B and A is defined by

$$\mathscr{C}_{BA}(\mathbf{q},t) = \mathrm{Tr}\{B_{\mathbf{q}}(t)A_{-\mathbf{q}}\hat{\rho}_{\mathrm{eq}}\}, \tag{2.8}$$

and the *propagator* is defined by

$$\mathscr{G}_{BA}(\mathbf{q},t) = \mathrm{Tr}\{B_{\mathbf{q}}(t)A_{-\mathbf{q}}\}. \tag{2.9}$$

It can be shown in a straightforward fashion that Φ_{BA} can be written as the Kubo transform of the response function of $B_{\mathbf{q}}$ and $A'_{-\mathbf{q}} \equiv dA_{-\mathbf{q}}/dt$:

$$\Phi_{BA}(\mathbf{q},t) = \hat{\Phi}_{BA'}(\mathbf{q},t). \tag{2.10}$$

We define $Z(\omega)$, the one-sided temporal Fourier transform of a function $\mathscr{Z}(t)$ by

$$Z(\omega) = \lim_{\eta\to 0}\int_0^\infty dt \exp[-i(\omega - i\eta)t]\mathscr{Z}(t). \tag{2.11}$$

The Fourier transforms of $\Phi_{BA}(\mathbf{q},t)$, $\hat{\Phi}_{BA}(\mathbf{q},t)$, $\mathscr{C}_{BA}(\mathbf{q},t)$, and $\mathscr{G}_{BA}(\mathbf{q},t)$ are denoted $\chi_{BA}(\mathbf{q},\omega)$, $\hat{\chi}_{BA}(\mathbf{q},\omega)$, $C_{BA}(\mathbf{q},\omega)$, and $G_{BA}(\mathbf{q},\omega)$, respectively. Performing the trace in Eqs. (2.6)–(2.9), and substituting the results in Eq. (2.11) yields

$$\chi_{BA}(\mathbf{q},\omega) = \sum_{\nu,\mu}\frac{(B_{\mathbf{q}})_{\nu\mu}(A_{-\mathbf{q}})_{\mu\nu}(P_\nu - P_\mu)}{\hbar(\omega - \omega_{\nu\mu} - i\eta)}, \tag{2.12a}$$

$$\hat{\chi}_{BA}(\mathbf{q},\omega) = -i\sum_{\nu,\mu}\frac{(B_{\mathbf{q}})_{\nu\mu}(A_{-\mathbf{q}})_{\mu\nu}(P_\nu - P_\mu)}{\hbar\omega_{\mu\nu}(\omega - \omega_{\nu\mu} - i\eta)}, \tag{2.12b}$$

$$C_{BA}(\mathbf{q},\omega) = -i\sum_{\nu,\mu}\frac{(B_{\mathbf{q}})_{\nu\mu}(A_{-\mathbf{q}})_{\mu\nu}P_\nu}{(\omega - \omega_{\nu\mu} - i\eta)}, \tag{2.12c}$$

$$G_{BA}(\mathbf{q},\omega) = -i\sum_{\nu,\mu}\frac{(B_{\mathbf{q}})_{\nu\mu}(A_{-\mathbf{q}})_{\mu\nu}}{(\omega - \omega_{\nu\mu} - i\eta)}. \tag{2.12d}$$

The indices ν and μ label the eigenstates of the unperturbed Hamiltonian H in Eq. (2.3). $\hbar\omega_{\nu\mu} = E_\nu - E_\mu$, where E_ν and E_μ are eigenvalues of H. $P_\nu = \langle\nu|\hat{\rho}_{\mathrm{eq}}|\nu\rangle$. Numerous useful relations among these four quantities can be obtained from Eqs. (2.12).[45–49] In the following discussion, we shall make use of the relationship between χ and $\hat{\chi}$, which can be derived from Eqs. (2.12a) and (2.12b):

$$\hat{\chi}_{BA}(\mathbf{q},\omega) = (i/\omega)[\chi_{BA}(\mathbf{q},\omega) - \chi_{BA}(\mathbf{q},0)]. \tag{2.13}$$

We divide the quantities in Eqs. (2.12) into real and imaginary parts according to

$$\Psi(\mathbf{q},\omega) = \Psi'(\mathbf{q},\omega) - i\pi\Psi''(\mathbf{q},\omega). \tag{2.14}$$

Application of the identity

$$(y - i\eta)^{-1} = P(1/y) + i\delta(y) \tag{2.15}$$

to Eqs. (2.12) yields the fluctuation–dissipation theorem

$$\chi''_{AA}(\mathbf{q},\omega) = \{[\exp(\beta\hbar\omega) - 1]/\hbar\}C'_{AA}, \tag{2.16}$$

and the Kramers–Kronig relations:

$$\chi'_{AA}(\mathbf{q},\omega) = (\pi^{-1})P\int_{-\infty}^{\infty} d\omega'\,\frac{\chi''_{AA}(\mathbf{q},\omega')}{\omega' - \omega}, \tag{2.17a}$$

$$\chi''_{AA}(\mathbf{q},\omega) = (\pi^{-1})P\int_{-\infty}^{\infty} d\omega'\,\frac{\chi'_{AA}(\mathbf{q},\omega')}{\omega - \omega'}. \tag{2.17b}$$

In Eqs. (2.15) and (2.17), P denotes the principle value.

For an isotropic fluid of charged particles, the electrical conductivity $\sigma(\mathbf{q},\omega)$ is defined by

$$\langle\mathscr{J}(\mathbf{q},\omega)\rangle = \sigma(\mathbf{q},\omega)E(\mathbf{q},\omega). \tag{2.18}$$

The current flux $\langle\mathscr{J}(\mathbf{q},\omega\rangle$ is the expectation value of $\mathscr{J}_{\mathbf{q}}$, the electric current operator in the presence of an electric field, which is related to $\rho_{\mathbf{q}}$, the operator that represents the particle density, and $\mathbf{J}_{\mathbf{q}}$, the particle current operator by[46]

$$\mathscr{J}_{\mathbf{q}} = \Omega^{-1}\left\{e\mathbf{J}_{\mathbf{q}} - (e^2/Mc)\sum_k \mathscr{A}_{\mathbf{k}}(t)\rho_{\mathbf{q}-\mathbf{k}}\right\}, \tag{2.19}$$

$$\mathbf{J}_{\mathbf{q}} = (2M)^{-1}\sum_m [\mathbf{p}_m \exp(i\mathbf{q}\cdot\mathbf{r}_m) + \exp(i\mathbf{q}\cdot\mathbf{r}_m)\mathbf{p}_m], \tag{2.20}$$

$$\rho_{\mathbf{q}} = \sum_m \exp(i\mathbf{q}\cdot\mathbf{r}_m). \tag{2.21}$$

M and e are the particle mass and charge, respectively, and Ω is the volume. $\mathbf{p}_m$ is the momentum operator for particle m. $\mathscr{A}_{\mathbf{k}}$ is the spatial Fourier transform of the vector potential of the external electromagnetic field. The density and current operators are related by the continuity equation, which is a consequence of the conservation of the number of particles:

$$\frac{\partial\rho_{\mathbf{q}}}{\partial t} = i\mathbf{q}\cdot\mathbf{J}_{\mathbf{q}}. \tag{2.22}$$

The conductivity is related to χ_{JJ}, the current–current response function, according to

$$\sigma(\mathbf{q},\omega) = ie^2/(\Omega\omega)[\chi_{JJ}(\mathbf{q},\omega) - \chi_{JJ}(\mathbf{q},0)]. \tag{2.23}$$

The current operator referred to in Eq. (2.23) is $\mathbf{J}_\mathbf{q}$, the current operator in the *absence* of an external field, which is defined in Eq. (2.20). Henceforth, "current operator" will be used to refer to this quantity, and not to $\mathcal{J}_\mathbf{q}$, the current operator in the *presence* of an external electric field, which is defined in Eq. (2.19). Comparison of Eqs. (2.13) and (2.23) shows that the electrical conductivity is proportional to the Kubo transformed current–current response function:

$$\sigma(\mathbf{q},\omega) = (e^2/\Omega)\hat{\chi}_{JJ}(\mathbf{q},\omega). \tag{2.24}$$

We are now able to relate $\sigma(\mathbf{q},\omega)$ to the density propagator $G_{\rho\rho}(\mathbf{q},\omega)$. We shall first derive an exact relation between $\sigma(\mathbf{q},\omega)$ and $C_{\rho\rho}$, and shall then construct an approximate relation between $C_{\rho\rho}$ and $G_{\rho\rho}$. In order to obtain a relation between σ and $C_{\rho\rho}$, we first express $\hat{\chi}_{JJ}$ in terms of $\chi_{\rho\rho}$, and then apply the fluctuation–dissipation theorem [Eq. (2.16)] to relate $\chi_{\rho\rho}$ to $C_{\rho\rho}$. Application of Eqs. (2.10) and (2.22) yields

$$iq\hat{\chi}_{JJ}(\mathbf{q},\omega) = \chi_{J\rho}(\mathbf{q},\omega). \tag{2.25}$$

$\chi_{J\rho}$ can be related to $\chi_{\rho\rho}$, by taking the Fourier transform of

$$\frac{\partial\Phi_{\rho\rho}(\mathbf{q},t)}{\partial t} = iq\Phi_{J\rho}(\mathbf{q},t) \tag{2.26}$$

to yield

$$i\omega\chi_{\rho\rho}(\mathbf{q},\omega) = iq\chi_{J\rho}(\mathbf{q},\omega). \tag{2.27}$$

In obtaining Eq. (2.27), we have made use of the fact that $\Phi_{\rho\rho}(\mathbf{q},0) = 0$. Combining Eqs. (2.24), (2.25), and (2.27) yields

$$\sigma(\mathbf{q},\omega) = ie^2\omega/(\Omega q^2)\chi_{\rho\rho}(\mathbf{q},\omega). \tag{2.28}$$

Application of the fluctuation–dissipation theorem [Eq. (2.16)] to Eq. (2.28) provides a relation between the real parts of the conductivity and the density–density correlation function:

$$\sigma'(\mathbf{q},\omega) = [(e^2\omega)/(\hbar\Omega q^2)][\exp(\beta\hbar\omega) - 1]C'_{\rho\rho}(\mathbf{q},\omega). \tag{2.29}$$

In order to relate σ'' to $C''_{\rho\rho}$, we use Eq. (2.28) to relate σ'' to $\chi'_{\rho\rho}$, the Kramers–Kronig relations to express $\chi'_{\rho\rho}$ in terms of $\chi''_{\rho\rho}$, the fluctuation–dissipation theorem to relate $\chi''_{\rho\rho}$ to $C'_{\rho\rho}$, and the Kramers–Kronig relations to express $C'_{\rho\rho}$ in terms of $C''_{\rho\rho}$. The final result is

$$\sigma''(\mathbf{q},\omega) = \frac{-e^2\omega}{q^2\pi^2\hbar\Omega} P\int_{-\infty}^{\infty}\frac{d\omega'}{\omega'-\omega}[\exp(\beta\hbar\omega') - 1] \times P\int_{-\infty}^{\infty}\frac{d\omega''}{\omega''-\omega'}C''_{\rho\rho}(\mathbf{q},\omega''). \tag{2.30}$$

Equations (2.29) and (2.30) represent the most general relation between $\sigma(\mathbf{q},\omega)$ and $C_{\rho\rho}(\mathbf{q},\omega)$. This relation assumes a much simpler form in the limit $\beta\hbar\omega \ll 1$. This condition, which corresponds to $\omega/T \ll 10^2$ GHz deg^{-1}, is usually satisfied in practice, since "high" frequencies in measurements of ac conductivities are often of the order of GHz. In this limit, we may linearize the exponential in the fluctuation–dissipation theorem [Eq. (2.16)], and therefore replace the factor $[\exp(\beta\hbar\omega') - 1]/\hbar$ in Eq. (2.30) with $\beta\omega'$. The integrals in Eq. (2.30) may then be carried out to yield

$$\sigma''(\mathbf{q},\omega) = -e^2\beta\omega/[\Omega q^2][\mathscr{C}_{\rho\rho}(\mathbf{q},0) - \omega C''_{\rho\rho}(\mathbf{q},\omega)]. \tag{2.31}$$

Taking the limit $\beta\hbar\omega \ll 1$ in Eq. (2.29) and combining that result with Eq. (2.31) provides a simple relation between σ and $C_{\rho\rho}$:

$$\sigma(\mathbf{q},\omega) = e^2\beta\omega/[\Omega q^2][i\mathscr{C}_{\rho\rho}(\mathbf{q},0) + \omega C_{\rho\rho}(\mathbf{q},\omega)]. \tag{2.32}$$

$K_{\rho\rho}$, the relaxation kernel of $C_{\rho\rho}$, is defined by

$$C_{\rho\rho}(\mathbf{q},\omega) = \mathscr{C}_{\rho\rho}(\mathbf{q},0)[i\omega + q^2K_{\rho\rho}(\mathbf{q},\omega)]^{-1}. \tag{2.33}$$

Substituting Eq. (2.33) into Eq. (2.32) yields

$$\sigma(\mathbf{q},\omega) = (e^2\beta/\Omega)\mathscr{C}_{\rho\rho}(\mathbf{q},0)\{i\omega K_{\rho\rho}(\mathbf{q},\omega)/[i\omega + q^2K_{\rho\rho}(\mathbf{q},\omega)]\}. \tag{2.34}$$

In an experimental determination of ac conductivity, the long wavelength limit of $\sigma(\mathbf{q},\omega)$ is measured:

$$\sigma(\omega) = \lim_{\mathbf{q}\to 0}\sigma(\mathbf{q},\omega). \tag{2.35}$$

This quantity is related to $K_{\rho\rho}$ by

$$\sigma(\omega) = (e^2\beta/\Omega)\mathscr{C}_{\rho\rho}(0,0)K_{\rho\rho}(0,\omega). \tag{2.36}$$

In the "high-temperature" limit ($\beta\hbar\omega \ll 1$), the complex ac conductivity is proportional to the relaxation kernel of the density–density correlation function.

We have rigorously established the relationship between $\sigma(\omega)$ and the kernel of the density–density *correlation function*. We next consider a set of approximations by which the ac conductivity can be related to the relaxation kernel of the density–density *propagator*, $G_{\rho\rho}(\mathbf{q},\omega)$ which is defined in Eq. (2.9):

$$G_{\rho\rho}(\mathbf{q},\omega) = [i\omega + q^2D(\mathbf{q},\omega)]^{-1}. \tag{2.37}$$

$D(\mathbf{q},\omega)$ is denoted the generalized diffusion kernel. If this quantity were independent of $\mathbf{q}$ and ω, then Eq. (2.37) would be the Green function of a diffusion equation with diffusion constant D. We next consider a class of models of disordered systems, of which the model treated in the subsequent sections is an example. The dynamics of N noninteracting charge carriers are described by a tight-binding Hamiltonian. The carriers may reside on any of N_s sites, which, on average, are identical. Let $\{|j\rangle\}$ be a set of orthonormal basis functions. In the state $|j\rangle$, a carrier resides at the site labeled j and located at position $\mathbf{r}_j$. For such a model, $\mathscr{C}_{\rho\rho}$ is given by

$$\mathscr{C}_{\rho\rho}(\mathbf{q},t) = \langle \mathrm{Tr}[\rho_\mathbf{q}(t)\rho_{-\mathbf{q}}\hat{\rho}_{\mathrm{eq}}]\rangle, \tag{2.38a}$$

$$\rho_\mathbf{q} = (N/N_s)\sum_{j=1}^{N_s}\exp(i\mathbf{q}\cdot\mathbf{r}_j)|j\rangle\langle j|. \tag{2.38b}$$

In Eq. (2.38a), Tr denotes a trace over the states $\{|j\rangle\}$, and the angular brackets denote an average over other degrees of freedom in the model. The angular brackets might, for example, represent a trace over phonon variables for a solid or solvent variables for a solution. The sum in Eq. (2.38b) runs over the N_s sites. [In the general expression for $\rho_\mathbf{q}$ in Eq. (2.21), the sum runs over the N carriers.] We then make a factorization approximation, and separately average the dynamic and static factors in Eq. (2.38a) over the solvent de-

grees of freedom:

$$\mathscr{C}_{\rho\rho}(\mathbf{q},t) = \mathrm{Tr}[\langle \rho_{\mathbf{q}}(t)\rho_{-\mathbf{q}}\rangle \langle \hat{\rho}_{\mathrm{eq}}\rangle]. \tag{2.39}$$

Since all sites are assumed to be identical, when averaged over the other degrees of freedom, $\langle \hat{\rho}_{\mathrm{eq}}\rangle$ is the unit matrix in the space spanned by the states $\{|j\rangle\}$, and $\mathscr{C}_{\rho\rho} = \mathscr{G}_{\rho\rho}$. For such a model, and within the factorization approximation of Eq. (2.39), the density–density *correlation function* [Eq. (2.33)] is identical to the density–density *propagator* [Eq. (2.37)], and hence $K_{\rho\rho} = D$. Under these conditions, $\mathscr{C}_{\rho\rho}(0,0) = N$, and the ac conductivity in Eq. (2.36) is proportional to the long-wavelength limit of the generalized diffusion kernel.

$$\sigma(\omega) = (N/\Omega)e^2\beta D(0,\omega). \tag{2.40}$$

This "generalized Einstein relation" was derived by Odagaki and Lax in the limit of high temperature for a class of models in which a carrier executes a random walk on an ordered array of sites with hopping rates that are random variables.[50] The present derivation applies to a more general class of quantum transport models, in which the carrier motion is not necessarily described by a hopping rate. Equation (2.40) will be used in the following sections to calculate the ac conductivity. We emphasize that the present theory is developed under the assumption that there are no interactions among the charge carriers. If such interactions are included, we expect local field corrections to be significant, especially on the insulating side of the metal–insulator transition.[51] A microscopic theory of the metal–insulator transition that incorporates local field effects remains to be developed.

III. MODE-COUPLING SELF-CONSISTENT EQUATION FOR CARRIER DYNAMICS

In this section, we treat a model of carrier transport in condensed phases that includes both dynamic and static sources of disorder. We develop a self-consistent equation for $D(\mathbf{q},\omega)$, the diffusion kernel of $G_{\rho\rho}(\mathbf{q},\omega)$, from which, according to the assumptions discussed at the end of the previous section, the ac conductivity may be calculated using Eq. (2.40). We consider a lattice in d dimensions with two types of sites: active sites on which the carriers may reside, and forbidden sites that are inaccessible to the carriers. A fraction c of the sites are active, and these sites are randomly distributed on the lattice. Since the carriers are assumed not to interact with each other, we consider the dynamics of a single carrier. For a given configuration of this random system, the single particle density matrix $\hat{\rho}$ obeys the Liouville equation:

$$\frac{d\hat{\rho}}{dt} = -i[H,\hat{\rho}], \tag{3.1}$$

$$H = \sum_m \omega_m(t)|m\rangle\langle m| + \sum_{m,n} J_{mn}|m\rangle\langle n|. \tag{3.2}$$

The sums in Eq. (3.2) run over the indices labeling the active sites. $|m\rangle$ denotes the state in which the carrier resides at the active site labeled m. J_{mn} is the transfer matrix element between active sites m and n, which we will take to have the value J if m and n are nearest neighbors on the lattice, and to vanish otherwise. $\hbar\omega_m(t)$ is a stochastic variable that represents the fluctuating site energy of the active site labeled m. By choosing ω_m to be a stochastic variable, we take into account, in a phenomenological way, the influence on the site energies of other degrees of freedom such as phonons that are not explicitly included in the model. The site energies are taken to be Gaussian stochastic variables, with an exponential correlation function that is characterized by a mean-squared amplitude Δ^2 and a correlation time Λ^{-1}:

$$\langle \omega_m(t)\omega_n(\tau)\rangle = \delta_{mn}\Delta^2 \exp(-\Lambda|t-\tau|). \tag{3.3}$$

If we set $c = 1$ (the ordered lattice limit), the present model reduces to a model that has been studied in the context of exciton dynamics in molecular crystals at finite temperature.[12,13] Neither the absorption spectrum nor transport properties can be determined exactly within this model, and approximate methods must be applied. The absorption spectrum has been calculated for this model by Sumi,[12] who used the coherent potential approximation, and by Blumen and Silbey,[13] who used a truncated cumulant expansion. A microscopic model of exciton dynamics with exciton–phonon coupling that is linear in the phonon coordinates can be mapped into the present problem in an approximate fashion, in which case the parameter Δ^2 is linear in the temperature, for kT large compared to lattice vibration energies.[12] It should be emphasized that the absorption line shape does not contain sufficient information to determine transport properties, and that the approximations that are used to calculate the line shape cannot in general be applied to determine $G_{\rho\rho}$. This model also includes a variety of other previously studied models as special cases, as discussed in the Introduction. These models include the Anderson model,[26–33] quantum percolation,[33–36] and the Haken–Strobl model.[7]

To determine $G_{\rho\rho}$ for the present model, we shall follow the mode-coupling procedure that has been applied to the quantum percolation model,[41] and to a model of transport in disordered systems that is based on a Pauli master equation.[39] In this approach, we focus on two transport properties: the diffusion kernel $D(\mathbf{q},\omega)$, and $\mathscr{P}_0(t)$, the averaged probability that a carrier that is located at a particular position at a given time is to be found at that position after the passage of time t. The diffusion kernel $D(\mathbf{q},\omega)$ is defined in Eq. (2.37). We shall find it convenient to work with the real quantity $D(\mathbf{q},-i\epsilon)$ (with ϵ real), rather than the complex quantity $D(\mathbf{q},\omega)$ (with ω real). We define $\hat{D}(\mathbf{q},\epsilon) \equiv D(\mathbf{q},-i\epsilon)$. $P_0(\epsilon)$ is the Laplace transform [$\omega = -i\epsilon$ in Eq. (2.11)] of $\mathscr{P}_0(t)$. Our goal is to construct a pair of coupled equations for $P_0(\epsilon)$ and $\hat{D}(\mathbf{q},\epsilon)$. $P_0(\epsilon)$ is related to the diffusion kernel by

$$P_0(\epsilon) = \frac{\Omega_0}{(2\pi)^d}\int d\mathbf{q}[\epsilon + q^2\hat{D}(\mathbf{q},\epsilon)]^{-1}. \tag{3.4}$$

The integration in Eq. (3.4) is carried out over the first Brillouin zone. Ω_0 is the volume of the unit cell.

Equation (3.4) is an exact relation between P_0 and D, which follows from the definitions of these quantities. In order to construct a closed self-consistent equation, we need another independent relation between these two quantities. We obtain such a relation by following the procedure presented in Refs. 39 and 41. We introduce the definition

$$\hat{D}(\mathbf{q},\epsilon) \equiv \tilde{D}[\mathbf{q},P_0(\epsilon)]. \tag{3.5}$$

In Eq. (3.5), $\hat{D}(\mathbf{q},\epsilon)$ is expressed as a functional of $P_0(\epsilon)$, which depends implicitly on ϵ through its dependence on P_0. Let us define a function F such that $P_0 = F(\epsilon)$. If the inverse of F exists, so that $\epsilon = F^{-1}(P_0)$, then any function of ϵ can be written as a functional of P_0. In particular $\hat{D}(\mathbf{q},\epsilon) = \hat{D}[\mathbf{q},F^{-1}(P_0)] \equiv \tilde{D}(\mathbf{q},P_0)$. Equation (3.5) should be regarded as a definition of the functional $\tilde{D}$. The only assumption underlying this definition is that F^{-1} exists. Since $\tilde{D}(\mathbf{q},P_0)$ cannot be determined exactly for the present model, we shall derive a hierarchy of approximations to this quantity [Eq. (3.8)]. An approximation to $\tilde{D}(\mathbf{q},P_0)$ provides a second independent relation between $\hat{D}(\mathbf{q},\epsilon)$ and $P_0(\epsilon)$, which, in combination with Eq. (3.4), yields a pair of coupled equations for these two quantities. $\tilde{D}$ is assumed to depend on c explicitly as well as depending on c implicitly through the dependence on c of P_0. We expand D with respect to its explicit dependence on c:

$$\tilde{D}(\mathbf{q},P_0) = \sum_{n=1}^{\infty} c^n \tilde{D}_n(\mathbf{q},P_0). \tag{3.6}$$

The coefficients $\tilde{D}_n$ in Eq. (3.6) depend on c only through the dependence on c of P_0. Each term in the expansion therefore depends on c to infinite order. Equations (3.5) and (3.6) should be regarded as a partially resummed density expansion of $\hat{D}(\mathbf{q},\epsilon)$. $\hat{D}(\mathbf{q},\epsilon)$ can also be expanded in an ordinary (not resummed) density expansion:

$$\hat{D}(\mathbf{q},\epsilon) = \sum_{n=0}^{\infty} c^n \hat{D}_n(\mathbf{q},\epsilon). \tag{3.7}$$

The coefficients $\hat{D}_n$ in Eq. (3.7) are independent of c. In Appendix A of Ref. 41, a procedure is given by which $\tilde{D}_n$ can be uniquely determined from $\hat{D}_j$ for $j \leqslant n$, and from the corresponding coefficients in the unresummed density expansion of P_0. The coefficients of c^m in the unresummed density expansions of $\hat{D}(\mathbf{q},\epsilon)$ and P_0 can be obtained from the exact values of these quantities for systems with j active sites, where $j \leqslant m+1$. The expansion in Eq. (3.6) can be truncated at order n to yield an approximation, $\tilde{D}^{(n)}$ that is exact to order n in c:

$$\hat{D}(\mathbf{q},\epsilon) \cong \tilde{D}^{(n)}(\mathbf{q},P_0) = \sum_{m=1}^{n} c^m \tilde{D}_m(\mathbf{q},P_0). \tag{3.8}$$

Equation (3.8) is an approximate relation between $\hat{D}(\mathbf{q},\epsilon)$ and P_0, which can be used to close Eq. (3.4). Equations (3.4) and (3.8) form a hierarchy of coupled equations for $\hat{D}(\mathbf{q},\epsilon)$ and P_0, whose solutions will be exactly correct to order c^n. In the present work, we shall consider the first member of this hierarchy, with $n = 1$. In Appendix A of Ref. 41, it is shown that $\tilde{D}_1(\mathbf{q},P_0) = \hat{D}_1[\mathbf{q},P_0^{-1}]$. As shown in Appendix B of Ref. 41, $\hat{D}_1$ can be determined from the solution to the transport problem with two active sites. The first member of the hierarchy of relations between $\hat{D}$ and P_0 in Eq. (3.8) is

$$q^2 \hat{D}(\mathbf{q},\epsilon) = cP_0^{-2} \sum_{r_{12}} [1 - \exp(i\mathbf{q}\cdot\mathbf{r}_{12})] G_{22,11}(P_0^{-1}). \tag{3.9}$$

$G_{22,11}(\epsilon)$ is the Laplace transform [$\omega = -i\epsilon$ in Eq. (2.11)] of $\mathcal{G}_{22,11}(t)$, which is the probability that for two active sites separated by a distance $\mathbf{r}_{12}$, a carrier that resides on site 1 at time zero can be found at site 2 at time t. We shall determine transport properties for the present model as follows. $G_{22,11}$ can be obtained from the solution of the two-site problem. Substitution of Eq. (3.9) into the denominator of Eq. (3.4) yields a closed equation for P_0, whose solution will be correct to order c. Substitution of this solution into the right-hand side of Eq. (3.9) gives $\hat{D}(\mathbf{q},\epsilon)$ as a function of ϵ, from which the propagator $G_{\rho\rho}$ can be obtained, using Eq. (2.37).

In order to evaluate Eq. (3.9), we need the exact solution to the two-site problem. The equation of motion of the density matrix $\hat{\rho}$ for the two-site problem is

$$\frac{\partial \hat{\rho}}{\partial t} = [A + B\omega_{12}(t)]\hat{\rho}, \tag{3.10a}$$

$$\omega_{12}(t) \equiv \omega_1(t) - \omega_2(t), \tag{3.10b}$$

$$\langle \omega_{12}(t)\omega_{12}(\tau)\rangle = 2\Delta^2 \exp(-\Lambda|t-\tau|), \tag{3.10c}$$

$$A_{11,12} = A_{22,21} = A^*_{11,21} = A^*_{22,12} = iJ,\ A_{ij,kl} = A_{kl,ij}, \tag{3.10d}$$

$$B_{12,12} = B^*_{21,21} = i. \tag{3.10e}$$

The density matrix for two sites has four components: $\hat{\rho}_{11}$, $\hat{\rho}_{12}$, $\hat{\rho}_{21}$, and $\hat{\rho}_{22}$, where $\hat{\rho}_{jj}$ represents the probability that the carrier resides at site j, and $\hat{\rho}_{jl}$ represents a coherence between sites j and l. The operators A and B are represented by 4×4 matrices with elements $A_{ij,kl}$ and $B_{ij,kl}$, where $i,j,k,l = 1,2$. The nonzero elements of the tetradic matrices A and B are given in Eqs. (3.10d) and (3.10e). The solution of Eq. (3.10a), averaged over the stochastic variables ω_1 and ω_2, is denoted by

$$\langle \hat{\rho}(t)\rangle = \mathcal{G}(t)\hat{\rho}(0). \tag{3.11}$$

Like the operators A and B in Eq. (3.10), $\mathcal{G}(t)$ can be represented as a 4×4 matrix. Equations (3.10) are identical to the equations of motion of a two level system with Gaussian frequency modulation in an electromagnetic field of arbitrary intensity.[52,53] The equation of motion in that problem is identical to Eq. (3.10a), if the Rabi frequency is replaced by $2J$, and the rate of population decay from level 2 to level 1 is set to zero. (The Rabi frequency is $\mu E/\hbar$, where μ is the transition dipole moment of the two-level system and E is the electric field amplitude.) The nonlinear optical properties of this model such as the absorption line shape and resonance fluorescence have been the subject of several studies.[52,53] It has been shown that the propagator $G(\epsilon)$ can be represented as a matrix continued fraction.[52,53] $G(\epsilon)$ is the Laplace transform of $\mathcal{G}(t)$ [$\omega = -i\epsilon$ in Eq. (2.11)]:

$$G(\epsilon) = [\epsilon - A - \Gamma(\epsilon)]^{-1}, \tag{3.12a}$$

$$\Gamma(\epsilon) = B\cfrac{2\Delta^2}{\epsilon + \Lambda - A - B\cfrac{4\Delta^2}{\epsilon + 2\Lambda - A - \cdots}B}B. \tag{3.12b}$$

Inspection of Eq. (3.12b) shows that the tetradic matrix $\Gamma(\epsilon)$ has at most four nonzero elements: $\Gamma_{12,12}(\epsilon)$, $\Gamma_{12,21}(\epsilon)$, $\Gamma_{21,12}(\epsilon)$ and $\Gamma_{21,21}(\epsilon)$. For convenience, we label these functions $\Gamma_1(\epsilon)$ through $\Gamma_4(\epsilon)$, respectively. Substitution of Eqs. (3.12) and (3.9) into Eq. (3.4) yields the

following pair of coupled equations for $P_0(\epsilon)$ and $\hat{D}(\mathbf{q},\epsilon)$:

$$P_0(\epsilon) = \{a^2/[2D(\epsilon)]\} I_d\{a^2\epsilon/[2D(\epsilon)]\}, \tag{3.13a}$$

$$D(\epsilon) = cD_0(P_0^{-1})/[1 + 2P_0D_0(P_0^{-1})a^{-2}], \tag{3.13b}$$

$$D_0(y) = (aJ)^2[\Gamma_1(y) + \Gamma_2(y) + \Gamma_3(y) + \Gamma_4(y)]/ [\Gamma_2(y)\Gamma_3(y) - \Gamma_1(y)\Gamma_4(y)], \tag{3.13c}$$

$$I_d(x) = \pi^{-d}\int_0^\pi dq_1 \cdots \int_0^\pi dq_d \left\{x + d - \sum_{n=1}^{d} \cos(q_n)\right\}^{-1}, \tag{3.13d}$$

$$q^2\hat{D}(\mathbf{q},\epsilon) = 2a^{-2}D(\epsilon)\left[d - \sum_{n=1}^{d} \cos(\mathbf{q}\cdot\mathbf{a}_n)\right]. \tag{3.13e}$$

$D(\epsilon)$ in Eqs. (3.13a) and (3.13b) is the $\mathbf{q}\to 0$ limit of $\hat{D}(\mathbf{q},\epsilon)$ in Eq. (3.13e). I_d is the diagonal element of the Green function for the d-dimensional analog of the simple cubic lattice.[25,54] The lattice vector in the direction n is $\mathbf{a}_n$, and has magnitude a. Equations (3.13) and (3.12) form the primary result of this work. Equations (3.13a) and (3.13b), can be solved for either $D(\epsilon)$ or for P_0. The solution for $D(\epsilon)$ can then be substituted into Eq. (3.13e) to yield $\hat{D}(\mathbf{q},\epsilon)$. Performing the analytic continuation $\epsilon = i\omega$ yields $D(\mathbf{q},\omega)$, from which $G_{\rho\rho}$ can be calculated according to Eq. (2.37).

IV. TRANSPORT PROPERTIES AT LONG TIMES AND SMALL FREQUENCIES

In order to solve Eqs. (3.13a) and (3.13b), the matrix elements Γ_1 through Γ_4 must be evaluated. For arbitrary values of Δ and Λ, Γ may be calculated numerically from the matrix continued fraction in Eq. (3.12b). We can, however, analytically determine the asymptotic behavior of the solution of Eqs. (3.13a) and (3.13b) at small frequencies, and hence long times. There are two cases to consider: $\Lambda > 0$ (dynamic fluctuations) and $\Lambda = 0$ (static site energy disorder). The small frequency (long time) behavior of the solution of Eqs. (3.13a) and (3.13b) is different in each of these cases. We begin by considering this small frequency behavior in one, two, and three dimensions for $\Lambda > 0$, in which case "small frequency" means $\epsilon \ll \Lambda$. We expect that for sufficiently small frequencies, $P_0^{-1} \ll \Lambda$. [We shall solve Eqs. (3.13) within this assumption, and it is easily verified that the resulting solution is consistent with this condition.] In this limit, the coupled equations for D and P_0 become

$$P_0(\epsilon) = \{a^2/[2D(\epsilon)]\} I_d\{a^2\epsilon/[2D(\epsilon)]\}, \tag{4.1a}$$

$$D(\epsilon) = cD_0(0)/[1 + 2P_0D_0(0)a^{-2}]. \tag{4.1b}$$

Inspection of Eq. (3.12b) shows that the limit $\Gamma(0)$ exists for $\Lambda > 0$. $D_0(0)$, which depends on Δ, Λ, and J, but not on P_0, can be expressed in terms of the matrix elements of $\Gamma(0)$ by setting $y = 0$ in Eq. (3.13c). The integral in Eq. (4.1a) can be performed exactly in one dimension ($d = 1$) to yield

$$I_1(x) = [x^2 + 2x]^{-1/2}. \tag{4.2}$$

Substitution of Eq. (4.2) into Eqs. (4.1), and solution of the resulting equations in the limit of small ϵ, yields

$$D(\epsilon) = (\epsilon a^2c^2/2)[1 + (1 + c^{-2})^{1/2}], \tag{4.3a}$$

$$P_0(\epsilon) = \epsilon^{-1}\{1 + 2c^2[1 + (1 + c^{-2})]^{1/2}\}^{-1/2}. \tag{4.3b}$$

Equation (4.3b) has the form $P_0 = \alpha\epsilon^{-1}$. Applying the Tauberian theorem for Laplace transforms[55] shows that $\mathscr{P}_0(t)$ decays to a finite asymptotic value (α) in the limit of large t, and hence that a carrier is on average confined to a finite volume around its starting point. According to Eq. (4.3a), $D \sim \epsilon$. Within the approximation that led to Eq. (2.40), the ac conductivity is proportional to $D(i\omega)$. Equation (4.3a) predicts a vanishing dc conductivity. According to Eqs. (4.3), carriers are localized in $d = 1$ for all values of the parameters in the model (c, J, Δ, Λ). The integral in Eq. (3.13d) cannot be evaluated in closed form in two dimensions. However, we can solve Eqs. (4.1) in the limit that $a^2\epsilon/2D(\epsilon) \ll 1$. (It can be easily verified *a posteriori* that this condition holds for small ϵ and c near 1.) For small values of its argument, I_2 takes the form[25,54]

$$I_2(x) \cong (2\pi)^{-1}\ln(x^{-1}). \tag{4.4}$$

Substitution of Eq. (4.4) into Eqs. (4.1) yields

$$D(\epsilon) = (a^2/2)\exp(2\pi c)\epsilon, \tag{4.5a}$$

$$P_0(\epsilon) = \epsilon^{-1}c\exp(-2\pi c). \tag{4.5b}$$

As in $d = 1$, $D(\epsilon) \sim \epsilon$, and $P_0 \sim \epsilon^{-1}$. Equations (4.5) predict that carriers are localized in $d = 2$ for all values of c, J, Δ, and Λ. The small frequency behavior of P_0 and D in $d = 3$ can be obtained with a similar analysis. For small values of its argument, I_3 is given by[54]

$$I_3(x) \cong I_3(0) - \pi^{-1}(x/2)^{1/2}, \tag{4.6a}$$

$$I_3(0) \cong 0.505\,462. \tag{4.6b}$$

Substitution of Eq. (4.6a) into Eqs. (4.1) yields the following solutions for $D(\epsilon)$ and $P_0(\epsilon)$:

$$D(\epsilon) = \begin{cases} a^2\epsilon/[2\pi(c^* - c)]^2 - \epsilon^2\{a^4/[8\pi^4D_0(0)(c^* - c)^5]\}, & c < c^* \\ D_0(0)(c - c^*), & c > c^* \\ [D_0(0)a/2\pi]^{2/3}\epsilon^{1/3}, & c = c^* \end{cases}, \tag{4.7}$$

$$P_0(\epsilon) = \begin{cases} [2c[\pi(c^* - c)]^2]\epsilon^{-1}, & c < c^* \\ a^2[2D_0(0)(c - c^*)]^{-1}\{c^* - (a/2\pi)[(c - c^*)D_0(0)]^{-1/2}\epsilon^{1/2}\}, & c > c^*. \\ [c^*/2][2\pi a^2/D_0(0)]^{-2/3}\epsilon^{-1/3}, & c = c^* \end{cases} \tag{4.8}$$

Equations (4.1) predict a metal–insulator phase transition at the critical point $c^* = I_3(0) \cong 0.505\,462$ in $d = 3$. The prediction of a metal–insulator transition in $d = 3$, but not in $d = 1$ or $d = 2$ is in agreement with the scaling theory of Anderson localization.[43,44] Under the assumptions outlined in Sec. II, we can determine σ, the ac conductivity, at small frequencies by performing the analytic continuation $\epsilon = i\omega$ in Eq. (4.7). For $c < c^*$, σ', the real part of the ac conductiv-

ity, vanishes as ω^2 for small frequencies, and for $c > c^*$, it reaches a finite value as ω approaches zero (the dc conductivity). At $c = c^*$, $\sigma' \sim \omega^{1/3}$. Applying the Tauberian theorem for Laplace transforms to Eq. (4.8) yields the following asymptotic, long time behavior for $\mathscr{P}_0(t)$:

$$\mathscr{P}_0(t) = \{2c[\pi(c^* - c)]^2\}, \quad c < c^*, \tag{4.9a}$$

$$\mathscr{P}_0(t) \sim (a^3/4\pi)[D_0(0)(c - c^*)]^{-3/2} t^{-3/2}, \quad c > c^*, \tag{4.9b}$$

$$\mathscr{P}_0(t) \sim [c^*/2]\ [2\pi a^2/D_0(0)]^{-2/3} t^{-2/3}, \quad c = c^*. \tag{4.9c}$$

For $c > c^*$, $\mathscr{P}_0(t)$ decays to a finite value at long times, at $c = c^*$ it decays to zero as $t^{-2/3}$, and for $c > c^*$, it decays to zero as $t^{-3/2}$, in agreement with scaling arguments.[56] Another transport property of interest, which we shall calculate in the next section, is $\langle r^2(t)\rangle$, the mean-squared-displacement of a carrier. $\langle r^2(\epsilon)\rangle$, the Laplace transform of this quantity, is related to $D(\epsilon)$ by

$$\langle r^2(\epsilon)\rangle = (2d/\epsilon^2) D(\epsilon). \tag{4.10}$$

From this relation and Eq. (4.7), we obtain the behavior of $\langle r^2(t)\rangle$ at long times:

$$\langle r^2(t)\rangle \sim \begin{cases} 6a^2/[2\pi(c^* - c)]^2, & c < c^* \\ 6D_0(0)(c - c^*)t, & c > c^* \\ 6[D_0(0)a/2\pi]^{2/3} t^{2/3}, & c = c^* \end{cases}. \tag{4.11}$$

For $c < c^*$, $\langle r^2(t)\rangle$ reaches a finite value at long time, indicating that carriers are trapped in a finite volume. For $c > c^*$, the carrier moves diffusively at long times, with $\langle r^2(t)\rangle$ that increases linearly in time. At $c = c^*$, $\langle r^2(t)\rangle \sim t^{2/3}$. The carriers are not trapped, but their motion is less efficient than ordinary diffusion. This phenomenon is referred to as weak localization[57] or anomalous diffusion.[58]

We have determined the long time and small frequency behavior of the transport properties calculated from Eqs. (4.1) for $\Lambda > 0$ in terms of $D_0(0)$, a function of J, Δ, and Λ. D_0 is defined in terms of the matrix elements of Γ in Eq. (3.13c). In general, these matrix elements must be determined numerically from the matrix continued fraction expression for Γ in Eq. (3.12b). However, D_0 can be determined in closed form in the limit $\Lambda \gg \Delta$. In this limit, the correlation time of the site energy fluctuations is small compared to the inverse magnitude of the fluctuations. Under these conditions, the continued fraction in Eq. (3.12b) can be truncated to yield $\Gamma(\epsilon) = 2(\Delta^2/\Lambda)B^2$. Substituting this result into Eq. (3.13c) yields $D_0(0)$ in the dynamic limit ($\Lambda \gg \Delta$):

$$D_0(0) = J^2 a^2 \Delta^2/\Lambda. \tag{4.12}$$

We next turn to the analysis of the solution of Eqs. (4.1) for $\Lambda = 0$, which we denote the static limit. In this limit, the site energies are static, random variables with a Gaussian distribution. In the absence of topological disorder, $c = 1$, this model reduces to the Anderson model of a lattice with random site energies.[26–33] In Eqs. (4.3)–(4.10), we expressed the small frequency and long time behavior of the transport properties for nonzero Λ, in terms of $D_0(0)$ [Eq. (3.13c)]. This quantity is undefined for $\Lambda = 0$, and the asymptotic behavior in this case is different from that for finite Λ. In the static limit, the matrix-continued fraction expression for the propagator in Eq. (3.12) converges increasingly slowly as the frequency ϵ is decreased, and this expression is therefore not convenient to analyze in this limit. Fortunately, this propagator can be simply determined in the static limit by calculating the propagator for a pair of sites with different energies and performing an average over the site energies. The result is

$$G_{22,11}(\epsilon) = \int_{-\infty}^{\infty} d\omega_1 \int_{-\infty}^{\infty} d\omega_2 F(\omega_1) F(\omega_2) [2J^2/\epsilon] \times [\epsilon^2 + 4J^2 + (\omega_1 - \omega_2)^2]^{-1}, \tag{4.13}$$

where $\hbar\omega_j$ is the energy of site j, and $F(\omega)$ is the frequency distribution. For the present model, this distribution is Gaussian:

$$F(\omega) = [2\pi\Delta^2]^{-1/2} \exp[-\omega^2/2\Delta^2]. \tag{4.14}$$

Substituting Eq. (4.14) into Eq. (4.13), performing the integration, and substituting the result into Eqs. (3.9) and (3.13e) yields the following expression for $D(\epsilon)$:

$$D(\epsilon) = [a^2 c \pi^{1/2}/2P_0][J/\Delta]^2 z^{-1} \exp(z^2)\mathrm{erfc}(z), \tag{4.15a}$$

$$z^2 \equiv [P_0^{-2} + 4J^2]/4\Delta^2. \tag{4.15b}$$

The complementary error function[59] is denoted by erfc in Eq. (4.15a). Equations (3.13a) and (4.15) form a pair of coupled equations for $D(\epsilon)$ and $P_0(\epsilon)$ in the static limit. The small frequency behavior of these quantities can be determined analytically by taking the limit $J^2 \gg P_0^{-2}$ in Eq. (4.15), in analogy with the derivation of Eqs. (4.1). We shall solve the coupled equations under this assumption, and it is easily verified that the resulting solution is consistent with this condition. In the limit that $J^2 \gg P_0^{-2}$, the coupled equations for $D(\epsilon)$ and $P_0(\epsilon)$ are

$$P_0(\epsilon) = \{a^2/[2D(\epsilon)]\} I_d\{a^2\epsilon/[2D(\epsilon)]\}, \tag{4.16a}$$

$$D(\epsilon) = [ca^2/2P_0(\epsilon)] H(J/\Delta)\{1 - [2P_0(\epsilon)]^{-2} \times [(2J^2)^{-1} + \Delta^{-2}(1 - H(J/\Delta))/H(J/\Delta)]\}, \tag{4.16b}$$

$$H(y) \equiv \pi^{1/2} y \exp(y^2)\mathrm{erfc}(y). \tag{4.16c}$$

Equations (4.16), from which the long time behavior of the transport properties can be determined for the static limit ($\Lambda = 0$), should be compared to Eqs. (4.1), which yield this behavior for dynamic disorder ($\Lambda > 0$). The behavior of the solution of Eqs. (4.16) at long times and small frequencies in one, two, and three dimensions can be determined analytically with the same approach that was applied to Eqs. (4.1), and which yielded Eqs. (4.3), (4.5), and (4.7)–(4.10). In $d = 1$ and $d = 2$, we find $D(\epsilon) \sim \epsilon$, and $P_0(\epsilon) \sim (\epsilon)^{-1}$ for all values of c, J, and Δ. Since $D(\epsilon) \sim \epsilon$, the dc conductivity is always zero. This behavior was also found for the case of dynamical disorder in Eqs. (4.3) and (4.5). Equations (4.16) predict that carriers are always localized in $d = 1$ and $d = 2$. In $d = 3$, Eqs. (4.16) can be solved in the vicinity of the critical point by expanding the integral I_3 in Eq. (4.16a) according to Eq. (4.6a). The result is

$$D(\epsilon)=\begin{cases} a^2\epsilon[2\pi H(J/\Delta)]^{-2}(c^*-c)^{-2}, & c<c^* \\ a^2 I_3(0)c^{-1/2}(c-c^*)^{1/2}[(2J^2)^{-1}+\Delta^{-2}(1-H(J/\Delta))/H(J/\Delta)]^{-1/2}, & c>c^*, \\ a^2\epsilon^{1/5}\{I_3(0)(2\pi)^{-1}[(2J^2)^{-1}+\Delta^{-2}(1-H(J/\Delta))/H(J/\Delta)]^{-1}\}^{2/5}, & c=c^* \end{cases} \tag{4.17a}$$

$$c^*=I_3(0)/H(J/\Delta). \tag{4.17b}$$

Comparison of Eqs (4.17) with Eqs. (4.7), which give the corresponding result for a dynamically disordered system, illustrates the differences in the long time behavior of systems with static and dynamic disorder. The coefficient of ϵ in the expression for $c<c^*$ in Eq. (4.17) is proportional to $(c-c^*)^{-2}$, as is the corresponding coefficient in Eq. (4.7). However, $D(0)$ for $c>c^*$, which is proportional to the dc conductivity, vanishes as $(c-c^*)^{1/2}$ in the static case, and as $(c-c^*)$ in the dynamic case. At the critical point, $D\sim\epsilon^{1/5}$ in the static case, while $D\sim\epsilon^{1/3}$ for dynamic disorder. A metal–insulator transition is predicted at the critical concentration $c^*=I_3(0)/H(J/\Delta)$, where H is defined in Eq. (4.16c). *The critical concentration is a function of the magnitude of the site energy disorder.* For $\Delta \ll J$ (weak energetic disorder), $H(J/\Delta)\cong 1$, and $c^*\cong I_3(0)\cong 0.5055$. c^* increases as the magnitude of the energetic disorder is increased. As Δ/J is increased, c^* increases without bound, according to Eq. (4.17b). Of course, c, the fraction of active sites cannot exceed unity. If Δ/J is sufficiently large that $c^*\geqslant 1$, then the dc conductivity will vanish for all physically realizable values of c. If $\Delta=0$, the present model reduces to the quantum percolation problem, which has been the subject of several recent studies.[33–36] Our estimate of $c^*\cong 0.5055$ for $\Delta=0$ should be compared with the following numerical estimates of the quantum percolation threshold on a simple cubic lattice: 0.45 (Ref. 33), 0.38 (Ref. 34), 0.47 (Ref. 35), and 0.70 (Ref. 36). In the case of dynamic disorder [Eqs. (4.6)–(4.7)], the critical concentration is $c^*=I_3(0)\cong 0.5055$, and is independent of J and Δ. In a dynamically disordered system, the carrier moves in a dynamically averaged potential on time scales that are long compared to Λ^{-1}, the correlation time of the fluctuations. Since the critical behavior in this case is determined by dynamics on time scales longer than this correlation time, the critical concentration does not depend on the magnitude of the fluctuations. The critical condition in Eq. (4.17b) can be regarded in two ways. One can imagine fixing c and tuning Δ through the transition, or fixing Δ and adjusting c. Figure 1(A) shows a phase diagram, calculated from Eq. (4.17b). To the left of the solid curve, the system is an insulator (zero dc conductivity), and to the right it is a conductor (finite dc conductivity). For $c<I_3(0)\cong 0.5055$, carriers are localized for any value of Δ. For $c>I_3(0)$, carriers are delocalized for $\Delta=0$, but a transition occurs as Δ is increased. The corresponding phase diagram for nonzero Λ is shown in Fig. 1(B) for comparison.

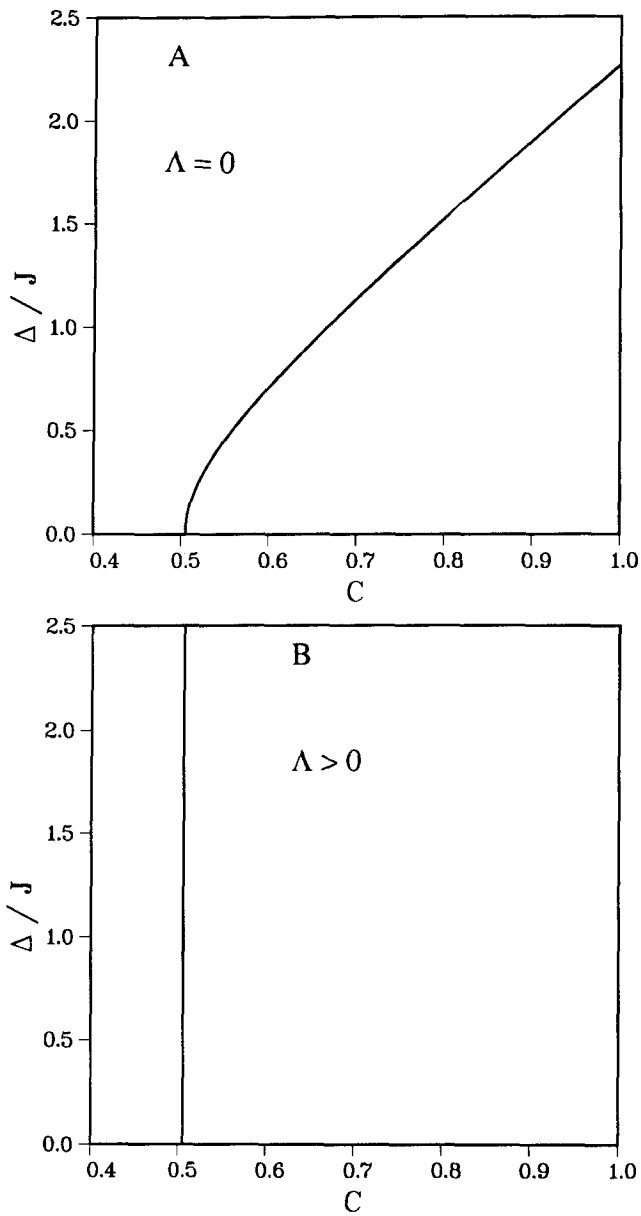

FIG. 1. (A) Phase diagram for a system with topological disorder, and static site energy disorder. Δ is the root-mean-squared site energy, J is the intersite interaction, c is the concentration of active sites. To the left of the solid curve, the system is an insulator (zero dc conductivity), and to the right of the solid curve it is a conductor (nonzero dc conductivity). (B) Phase diagram for a system with topological disorder and dynamic site energy disorder characterized by a finite correlation time Λ^{-1}. For $c>c^*\cong 0.5055$, the system is a conductor, and for $c<c^*$, it is an insulator. c^* does not depend on Δ/J, because for times long compared to Λ^{-1}, the carriers move in a dynamically averaged potential.

At $c=1$ there is no topological disorder, and the present model in the static limit reduces to the much studied Anderson model of a regular lattice with static, site energy disorder.[26–33] In the Anderson model, the distribution of site energies is taken to be rectangular rather than Gaussian. In order to compare with previous results, we have calculated the critical condition in Eq. (4.17b) for such a distribution by replacing Eq. (4.14) with

$$F(\omega)=\begin{cases} W^{-1}, & |\omega|\leqslant W/2 \\ 0, & |\omega|>W/2 \end{cases}. \tag{4.18}$$

The result is

$$c^* = I_3(0)/\mathcal{H}(J/W), \tag{4.19a}$$

$$\mathcal{H}(J/W) = 4(J/W)\tan^{-1}(W/2J) - (4J^2/W^2)\ln[1 + W^2/4J^2]. \tag{4.19b}$$

Setting $c^* = 1$ in Eq. (4.19a) and solving for W/J yields a prediction of the critical point in the Anderson model of $(W/J)^* \cong 7.5$. Recent numerical calculations of Anderson localization[28–33] on a simple cubic lattice yield values of $(W/J)^*$ that range from 14.5 to 19. It should be noted that the numerical methods that are expected to yield accurate values of critical points and exponents, such as renormalization group techniques, do not yield information on noncritical dynamics (dynamics at short or intermediate time or not near the critical point) as does the present analytical theory.

In this section, we have analyzed the long time behavior of the transport properties calculated from Eqs. (3.13), and have elucidated the critical dynamics. Such an asymptotic analysis does not tell us, however, exactly when this limiting behavior is attained. Estimation of this time is essential in order to determine whether the asymptotic analysis is relevant for a given measurement with a given experimental time scale.[60,61] In order to determine the time regime in which the asymptotic results are valid, one must solve Eqs. (3.13) for a wide range of times. Such numerical calculations are presented in the following section.

V. CALCULATION OF TRANSPORT PROPERTIES

In this section, we present calculations of $\mathcal{P}_0(t)$, the probability that a carrier is to be found at the initial site after a time t, $\langle r^2(t)\rangle$, the mean-squared displacement of a carrier, and $\sigma(\omega)$, the ac conductivity. These quantities are determined numerically with the following procedure. Substitution of the right-hand side of Eq. (3.13b) into the right-hand side of Eq. (3.13a) yields a closed equation for

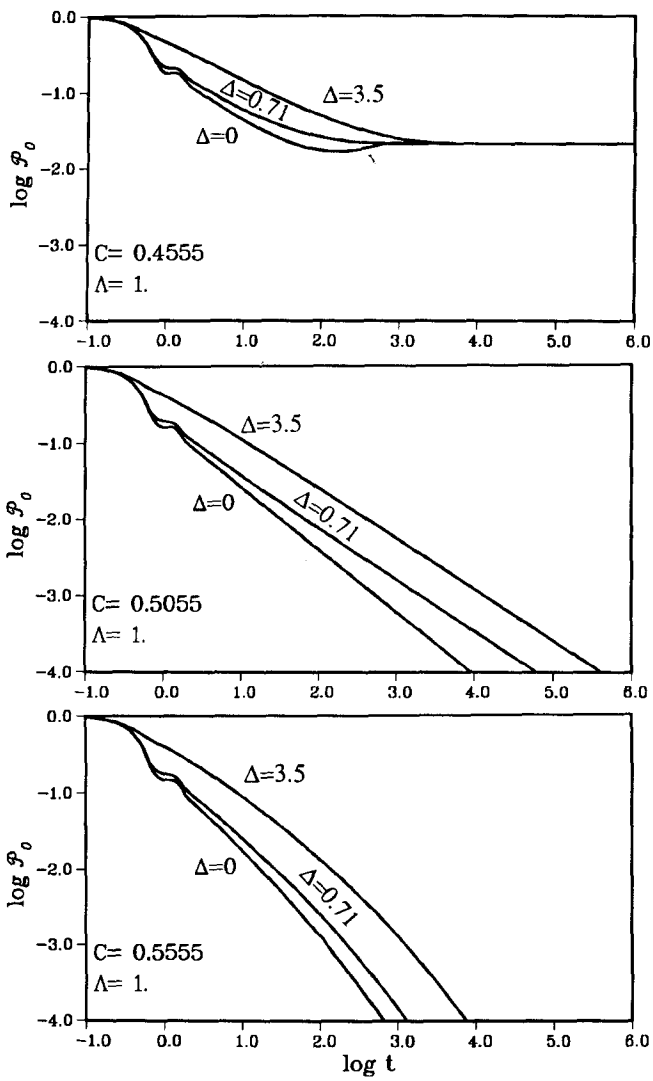

FIG. 2. $\mathcal{P}_0(t)$, the time dependent probability that a carrier can be found at the initital site after a time t, is shown for a range of values of Δ, the root-mean-squared magnitude of the site energy fluctuations, and c, the concentration of active sites. Λ, the inverse correlation time of the fluctuations, equals 1. All frequencies are measured in units of J, the intersite coupling, and the time is measured in units of J^{-1}. The metal–insulator transition occurs at $c = c^* \cong 0.5055$.

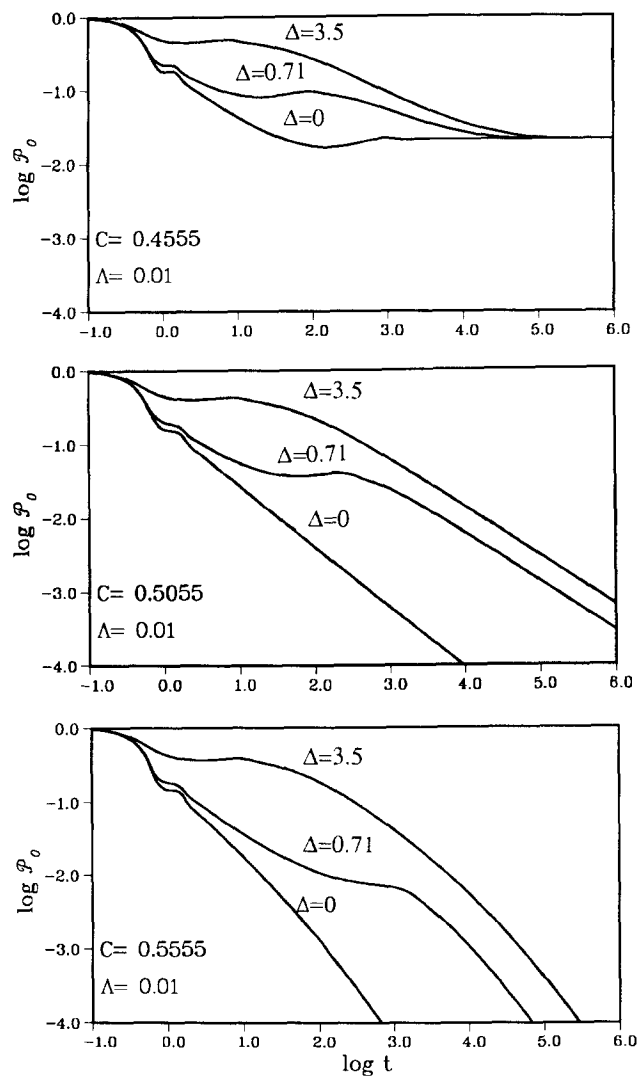

FIG. 3. $\mathcal{P}_0(t)$, the time-dependent probability that a carrier can be found at the initial site after a time t, is shown for $\Lambda = 0.01$ and the same values of c and Δ used in Fig. 2. Δ, the root-mean-squared magnitude of the site energy fluctuations, and Λ, the inverse correlation time of the fluctuations, are expressed in units of J, the intersite coupling, and t is expressed in units of J^{-1}.

$P_0(\epsilon)$, the Laplace transform of $\mathscr{P}_0(t)$. The integral $I_3(x)$, which is defined in Eq. (3.13d) cannot be evaluated in closed form. Two of the three nested integrations can be carried out to give a one-dimensional integral over an integrand containing a complete elliptic integral of the first kind.[25] The resulting equation is then solved numerically to give $P_0(\epsilon)$. [Solution of this equation involves evaluating the matrix continued fraction in Eq. (3.12). For the parameters used in this section, the continued fraction converges to 12 decimal places within 1000 steps.] $\mathscr{P}_0(t)$ is obtained by inverting the Laplace transform numerically, using the Stehfest algorithm.[62] Substitution of $P_0(\epsilon)$ into the right side of Eq. (3.13b) gives an explicit expression for $D(\epsilon)$, the small wave vector limit of the diffusion kernel. $\langle r^2(\epsilon)\rangle$, the Laplace transform of $\langle r^2(t)\rangle$, is related to $D(\epsilon)$ in Eq. (4.10). A numerical inverse Laplace transform then yields $\langle r^2(t)\rangle$. In Sec. II, we considered a set of approximations that led to Eq. (2.40), in which $\sigma(\omega)$ is proportional to $D(0,\omega)$. In principle $D(0,\omega)$ can be obtained from $D(\epsilon)$, by making the analytic continuation $\epsilon = i\omega$. Since Eqs. (3.13a) and (3.13b) do not yield a solution for $D(\epsilon)$ in closed form, we instead invert the Laplace transform in $D(\epsilon)$ to give a function of time, and then perform a fast Fourier transform (FFT) to obtain $D(0,\omega)$. The behavior of $D(0,\omega)$ for small ω, when calculated in this fashion, depends on the length of the time interval that was used in the FFT. In choosing this time interval, we made use of the fact that $D(0,\omega)$ at $\omega = 0$ equals $D(\epsilon)$ at $\epsilon = 0$. The time interval used in the FFT was chosen to minimize the numerical discrepancy between these quantities. The Laplace inversion was performed using 16 frequency points per time point.[62] For a given set of c, Λ, and Δ, the inverse Laplace transform of $D(\epsilon)$ was evaluated at 100 time points, and a cubic spline interpolation algorithm was used to provide up to 2^{13} points for the FFT.

Calculations of $\mathscr{P}_0(t)$ for a simple cubic lattice are shown in Figs. 2–4 for different values of Λ, the inverse correlation time of the site energy fluctuations, Δ, the root-

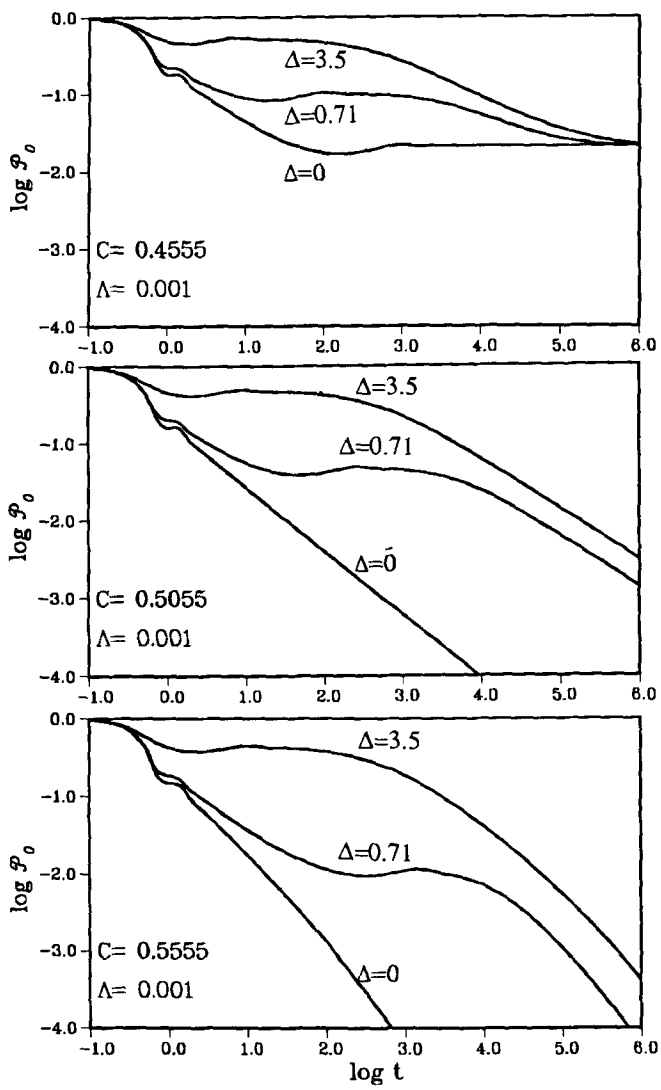

FIG. 4. $\mathscr{P}_0(t)$, the time-dependent probability that a carrier can be found at the initial site after a time t, is shown for $\Lambda = 0.001$ and the same values of c and Δ used in Figs. 2 and 3. Δ, the root-mean-squared magnitude of the site energy fluctuations, and Λ, the inverse correlation time of the fluctuations, are expressed in units of J, the intersite coupling, and t is expressed in units of J^{-1}.

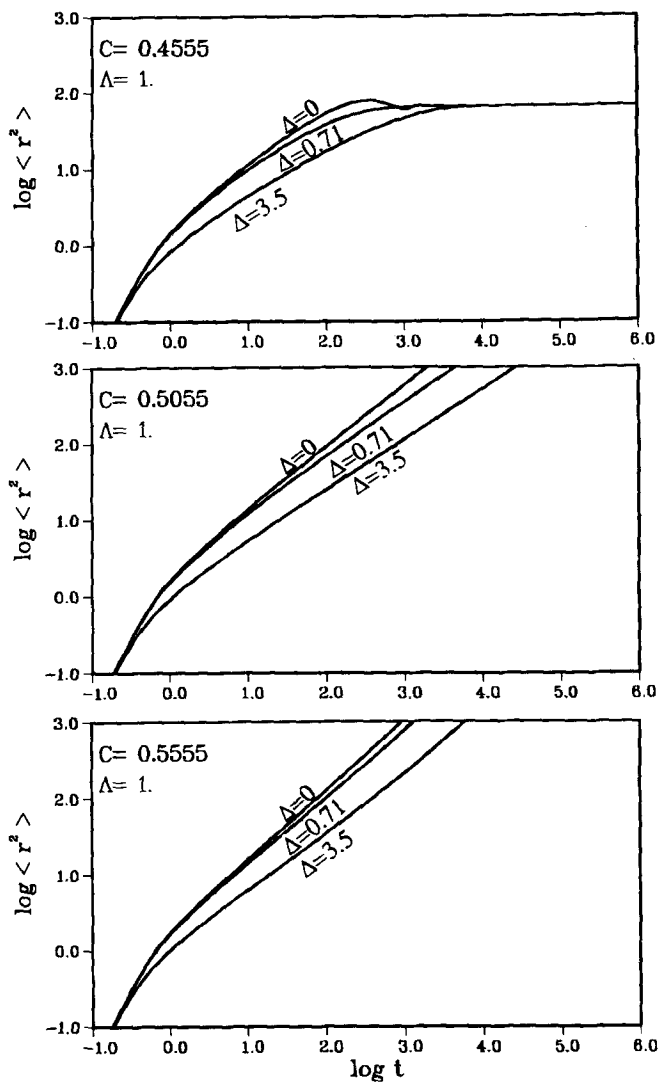

FIG. 5. $\langle r^2(t)\rangle$, the mean-squared displacement of the carrier, is shown for $\Lambda = 1$, and the same values of c and Δ used in Figs. 2–4. Δ, the root-mean-squared magnitude of the site energy fluctuations, and Λ, the inverse correlation time of the fluctuations, are expressed in units of J, the intersite coupling, and t is expressed in units of J^{-1}.

mean-squared magnitude of the fluctuations, and c, the concentration of active sites. Δ and Λ are given in units of J, the intersite interaction. In Figs. 2–4, $\Lambda = 1.0$, 0.01, and 0.001, respectively. Each figure shows $\mathscr{P}_0(t)$ for three concentrations: 0.4555 (below the critical point), 0.5055 (the critical point), and 0.5555 (above the critical point). For each concentration, $\mathscr{P}_0(t)$ is shown for $\Delta = 0$, 0.71, and 3.5. The time is measured in units of J^{-1}. Figures 2–4 show that $\mathscr{P}_0(t)$ decays to a finite value at long times for $c < c^*$, indicating that the carriers are localized in a finite volume. For $c \geqslant c^*$, $\mathscr{P}_0(t)$ decays to zero, and carriers can explore the entire volume. The long time behavior of $\mathscr{P}_0(t)$ was determined analytically in Eq. (4.9). It should be noted that the asymptotic analysis that led to Eq. (4.9) is valid only for $\Lambda > 0$, and hence does not apply to the calculations with $\Delta = 0$ (no site energy fluctuations). Inspection of Eq. (4.9) shows that the behavior of $\mathscr{P}_0(t)$ at long times depends only on c and not on Λ and Δ. Figures 2–4 confirm this behavior and illustrate that the time scale on which the asymptotic result is valid is strongly dependent on Λ and Δ. The times for which the asymptotic behavior holds become longer as Λ is decreased or as Δ is increased. In accordance with Eq. (4.9), $\mathscr{P}_0(t) \sim t^{-3/2}$ for $c = 0.5555$, and $\mathscr{P}_0(t) \sim t^{-2/3}$ at $c = 0.5055$, for $\Delta > 0$.

Figures 5–7 depict $\langle r^2(t) \rangle$ for the same set of parameters that was used in Figures 2–4. For $c > c^*$, $\langle r^2(t) \rangle$ increases linearly with time, for $c < c^*$, it reaches a finite value at long times, and at $c = c^*$, it increases less strongly than linearly in time, in agreement with the asymptotic behavior given in Eq. (4.11). Like Figs. 2–4, Figs. 5–7 show that the times for which the asymptotic analysis in Eq. (4.11) is valid increase with increasing Δ and decreasing Λ. For a given concentration and at a given time $\langle r^2(t) \rangle$ decreases as Δ increases. It is intuitively reasonable that carrier motion should become slower as the magnitude of the site energy fluctuations is increased. The consequence of the finite correlation time of the fluctuations is illustrated dramatically in Fig. 7 in the calculation for $c = 0.5555$, $\Lambda = 0.001$, and

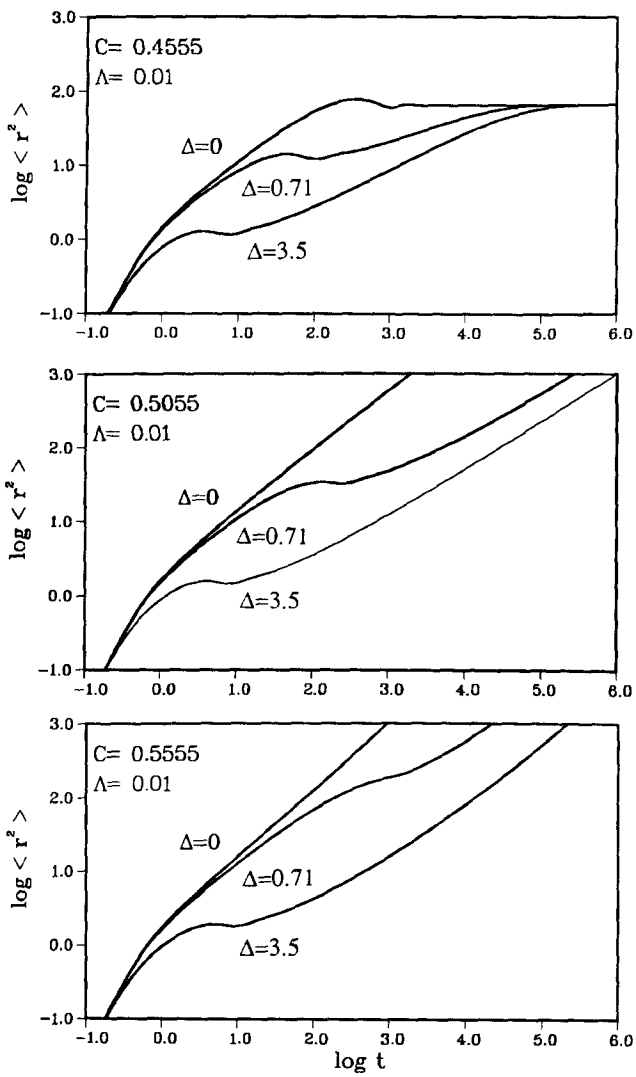

FIG. 6. $\langle r^2(t) \rangle$, the mean-squared displacement of the carrier, is shown for $\Lambda = 0.01$, and the same values of c and Δ used in Figs. 2–5. Δ, the root-mean-squared magnitude of the site energy fluctuations, and Λ, the inverse correlation time of the fluctuations, are expressed in units of J, the intersite coupling, and t is expressed in units of J^{-1}.

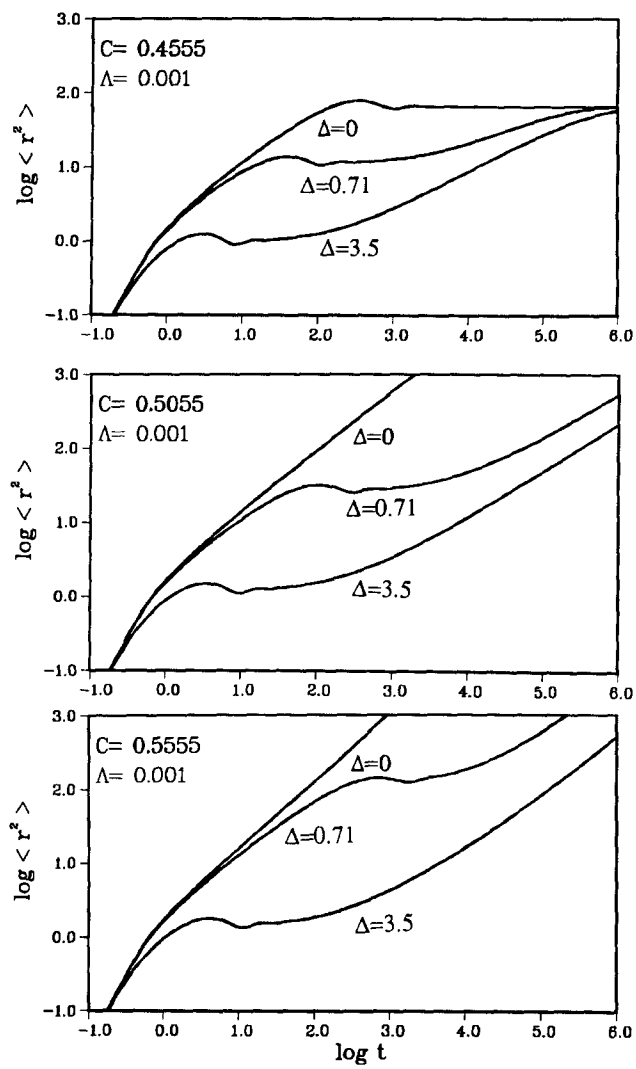

FIG. 7. $\langle r^2(t) \rangle$, the mean-squared displacement of the carrier, is shown for $\Lambda = 0.001$, and the same values of c and Δ used in Figs. 2–6. Δ, the root-mean-squared magnitude of the site energy fluctuations, and Λ, the inverse correlation time of the fluctuations, are expressed in units of J, the intersite coupling, and t is expressed in units of J^{-1}.

$\Delta = 3.5$. Since $c > c^*$, $\langle r^2(t)\rangle$ must increase linearly with time for long times, and such behavior is seen for $t \gg \Lambda^{-1}$. However, for a range of times less than Λ^{-1}, $\langle r^2(t)\rangle$ oscillates and does not grow appreciably. In an experiment carried out on that time scale, the carrier would appear to be localized.

According to Eq. (2.40), the ac conductivity $\sigma(\omega)$ is proportional to $D(0,\omega)$. The concentration dependence of $\sigma'(\omega)$, the real part of the ac conductivity, at two frequencies is illustrated in Figs. 8(A) and 8(B). [The prefactor in Eq. (2.40), $\beta e^2(N/\Omega)$, is set to unity.] Figure 8(A) shows the concentration dependence of $\sigma'(0)$, the real part of the dc conductivity. For $c > c^*$, the dc conductivity is nonzero, and for $c < c^*$, it vanishes. The sensitivity of $\sigma'(0)$ to Δ, the magnitude of the fluctuations, is clearly illustrated. The dc conductivity decreases as Δ increases for $c > c^*$. Figure 8(B) shows the concentration dependence of $\sigma'(\omega)$ evaluated at $\omega = J$, the intersite coupling frequency. Although $\sigma'(\omega)$ is never zero for $\omega > 0$, the curves in Fig. 8(B) display an abrupt increase with increasing concentration that is reminiscent of the critical behavior shown in Fig. 8(A). Thus, although a critical point does not exist in a formal sense for $\sigma'(\omega)$ at finite frequencies, this quantity does show an abrupt change as a function of concentration, which, if measured experimentally, would resemble critical behavior. The frequency dependence of $\sigma'(\omega)$ for different values of Δ is shown in Fig. 9 for $c = 0.7$ (above the transition) and for $c = 0.4$ (below the transition). For $c = 0.4$, $\sigma'(\omega)$ vanishes

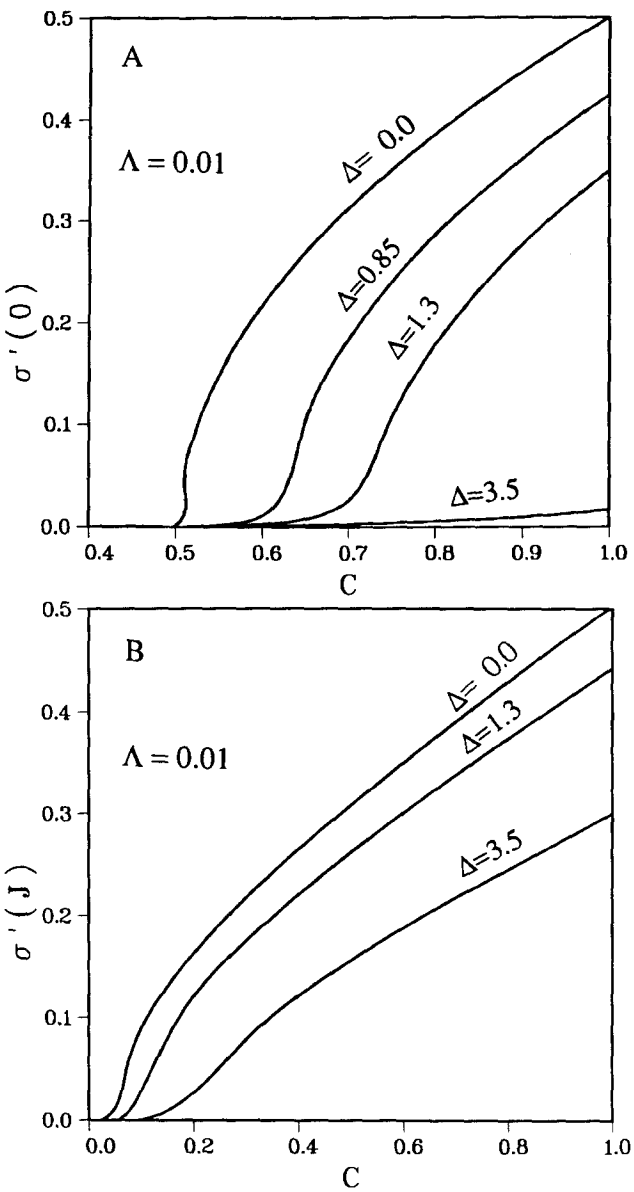

FIG. 8. (A) The concentration dependence of the real part of the dc conductivity is shown for $\Lambda = 0.01$ and four values of Δ. The dc conductivity vanishes for $c < c^*$, and is nonzero for $c > c^*$. $c^* \cong 0.5055$. Δ, the root-mean-squared magnitude of the site energy fluctuations, and Λ, the inverse correlation time of the fluctuations, are expressed in units of J, the intersite coupling. (B) The concentration dependence of the real part of the ac conductivity evaluated at $\omega = J$, is shown for the same parameters used in (A). $\sigma'(J)$ is nonzero for $c > 0$, but still shows an abrupt increase with increasing concentration that resembles a critical point.

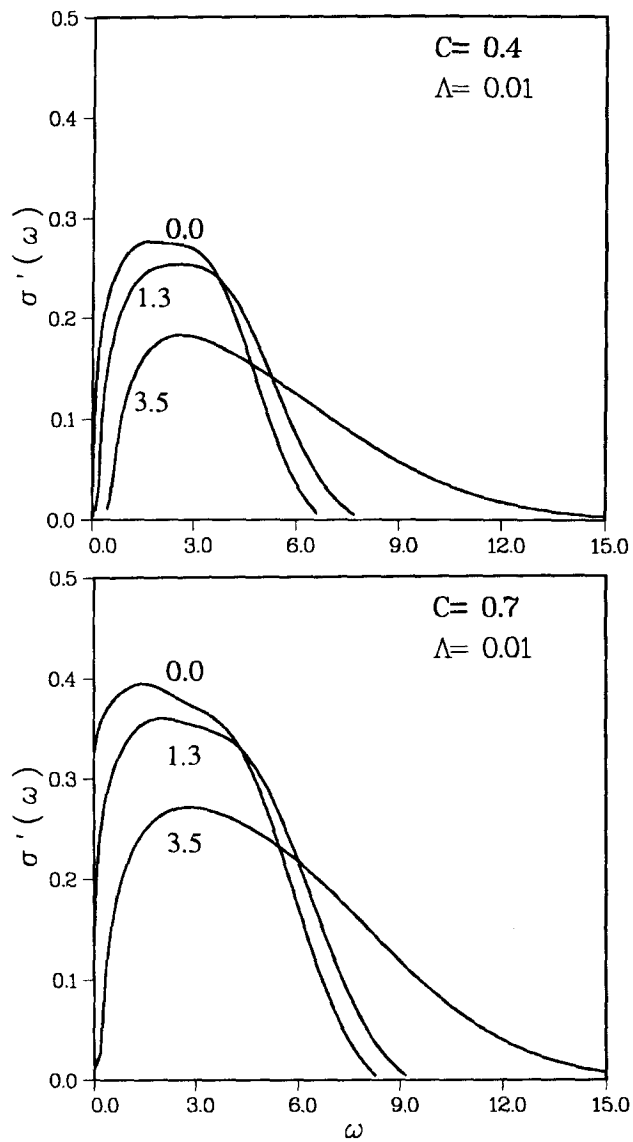

FIG. 9. The frequency dependence of the real part of the ac conductivity is shown for $c = 0.7$ (above the critical concentration) and $c = 0.4$ (below the critical concentration). $\Lambda = 0.01$. Each curve is labeled with the value of Δ. Δ, the root-mean-squared magnitude of the site energy fluctuations Λ, the inverse correlation time of the fluctuations, and ω are expressed in units of J, the intersite coupling.

at $\omega = 0$, and at $c = 0.7$, it attains a finite value in this limit. Comparison of these calculations shows that despite this important difference in the small frequency behavior of $\sigma'(\omega)$, the dependence of $\sigma'(\omega)$ at large frequencies for fixed Δ is qualitatively similar for $c > c^*$ and $c < c^*$.

VI. SUMMARY AND CONCLUSIONS

In this work we have treated a very general model of the motion of a carrier or electronic excitation in a condensed phase system, which includes topological disorder (the sites are randomly distributed in space), and energetic disorder that is characterized by an arbitrary correlation time Λ^{-1}. This model is extremely rich, and contains the Anderson model,[26–33] quantum percolation,[33–36] the Haken–Strobl model,[7] and coherent and incoherent motion[19] as limiting cases for various ranges of the parameters Δ, Λ, J, and c. A catalog of these limiting cases is given in the Introduction. We have derived a mode-coupling self-consistent equation for the density propagator [Eq. (3.13)] from which we have calculated the ac conductivity, the mean-squared-displacement of a carrier, and the time-dependent probability of finding a carrier at the initial site. A metal–insulator transition is predicted in three dimensions, but not in one or two dimensions, in agreement with scaling arguments.[43,44] The critical behavior predicted for $\Lambda = 0$ (static energy disorder) differs from that predicted for $\Lambda > 0$ (dynamic energy disorder). The difference in critical exponents for these two cases can be seen by comparing Eqs. (4.7) and (4.17). In the dynamic case, the critical behavior occurs on times that are long compared to Λ^{-1}. On such time scales, a carrier moves in a dynamically averaged potential. The existence or absence of a finite dc conductivity is determined only by the concentration of active sites. By contrast, in the static limit of $\Lambda = 0$, the existence of a finite dc conductivity depends on the width of the distribution of site energies, as well as on the concentration of active sites. In addition to analyzing the critical dynamics, we have performed numerical calculations of transport properties over a wide range of times and frequencies. These calculations illustrate the behavior of a carrier when there is not a separation of time scales between the dynamics of the carrier and those of the solvent. If the time associated with the motion of the carrier from site to site is small compared to the correlation time of the solvent, a carrier may be trapped in a finite volume for a time that is long compared to the time associated with site-to-site motion, but can eventually explore the entire system for times long compared to the correlation time of the solvent.

The present work constitutes the first analytical theory of transport in a medium that is characterized both by dynamic disorder with an arbitrary correlation time and by topological disorder. Each of these types of disorder plays an important role in the dynamics of excess electrons and other charge carriers in solution. The conductivity of excess electrons in liquid halogens has been studied recently by Gileadi and co-workers[3] and by Ludwig, Duppen, and Kommandeur[2], who have measured dc conductivities in these systems. Ludwig *et al.*[2] interpret their measurements on excess electrons in I_2 as follows. At low concentrations of electrons, each electron is delocalized over a cluster of approximately 100 I_2 molecules, and moves from cluster to cluster through fluctuations in solvent density. The present model constitutes an approximate representation of this scenario. Each "site" in the model can be taken to represent an I_2 cluster, and the fluctuating site energies represent the fluctuating binding energies of the electron to the cluster. The present calculations indicate the kind of information that could be obtained from ac conductivity measurements of excess electrons in solution. Measurements of the dc conductivity provide information on carrier dynamics at very long times, while ac measurements can probe a range of microscopically interesting time scales. We hope that this work may motivate such measurements.

ACKNOWLEDGMENTS

The support of the National Science Foundation, the Office of Naval Research, the U. S. Army Research Office, and the donors of the Petroleum Research Fund, administered by the American Chemical Society, is gratefully acknowledged.

[1]Proceedings of the Sixth International Conference on Excess Electrons and Metal-Ammonia Solutions, Colloque Weyl VI [J. Phys. Chem. **88**, 3699 (1984)].
[2]J. Ludwig, K. Duppen, and J. Kommandeur, J. Chem. Soc. Faraday Trans. 1 **80**, 2943 (1984).
[3]I. Rubenstein, M. Bixon, and E. Gileadi, J. Phys. Chem. **84**, 715 (1980).
[4]G. A. Kenney-Wallace and C. D. Jonah, J. Phys. Chem. **86**, 2572 (1982).
[5]C. A. Angell, Solid State Ionics **9**, 3 (1983).
[6]S. D. Druger, M. A. Ratner, and A. Nitzan, Phys. Rev. B **31**, 3939 (1985).
[7]H. Haken and G. Strobl, Z. Phys. **262**, 135 (1973).
[8]H. A. Kramers, Physica **7**, 284 (1940).
[9]S. H. Courtney and G. R. Fleming, J. Chem. Phys. **83**, 215 (1985); G. R. Fleming, *Chemical Applications of Ultrafast Spectroscopy* (Oxford University, Oxford, 1986), p. 179.
[10]R. F. Grote and J. T. Hynes, J. Chem. Phys. **73**, 2715 (1980).
[11]B. Bagchi and D. W. Oxtoby, J. Chem. Phys. **78**, 2735 (1983).
[12]H. Sumi, J. Chem. Phys. **67**, 2943 (1977).
[13]A. Blumen and R. Silbey, J. Chem. Phys. **69**, 3589 (1978).
[14]M. K. Grover and R. Silbey, J. Chem. Phys. **53**, 2099 (1970).
[15]R. Silbey and R. W. Munn, J. Chem. Phys. **72**, 2763 (1980).
[16]H. Mueller and P. Thomas, Phys. Rev. Lett. **51**, 702 (1983).
[17]S. M. Girvin and M. Jonson, Phys. Rev. B **22**, 3583 (1980).
[18]T. Holstein, Ann. Phys. (N.Y.) **8**, 343 (1959).
[19]V. M. Kenkre, in *Exciton Dynamics in Molecular Crystals and Aggregates*, edited by G. Hohler (Springer, Berlin, 1982).
[20]A. L. Nichols and D. Chandler, J. Chem. Phys. **84**, 398 (1986).
[21]B. Velicky, Phys. Rev. **184**, 614 (1969).
[22]R. Parson and R. Kopelman, Chem. Phys. **89**, 265 (1984).
[23]S. Abe and Y. Toyozawa, J. Phys. Soc. Jpn. **50**, 2185 (1981).
[24]A. K. Harrison and R. Zwanzig, Phys. Rev. A **32**, 1072 (1985).
[25]E. N. Economou, *Green's Functions in Quantum Physics* (Springer, Berlin, 1983).
[26]P. W. Anderson, Phys. Rev. **109**, 1492 (1958).
[27]R. Abou-Chacra, P. W. Anderson, and D. J. Thouless, J. Phys. C **6**, 1734 (1973).
[28]A. Singh and W. L. McMillan, J. Phys. C **17**, 2097 (1985).
[29]D. C. Licciardello and E. N. Economou, Phys. Rev. B **11**, 3697 (1975).
[30]J. L. Pichard and G. Sarma, J. Phys. C **14**, L617 (1981).
[31]A. MacKinnon and B. Kramer, Z. Phys. B **53**, 1 (1983).
[32]S. Sarker and E. Domany, Phys. Rev. B **23**, 6018 (1983).
[33]L. Root and J. L. Skinner, Phys. Rev. B **33**, 7738 (1986).
[34]R. Raghavan, Phys. Rev. B **29**, 748 (1984).
[35]V. Srivastava and M. Chaturvedi, Phys. Rev. B **30**, 2238 (1984).
[36]T. Odagaki and K. C. Chang, Phys. Rev B **30**, 1612 (1984).
[37]R. F. Loring, H. C. Andersen, and M. D. Fayer, J. Chem. Phys. **80**, 5731 (1984).
[38]J. Nieuwoudt and S. Mukamel, Phys. Rev. B **30**, 4426 (1984).

[39]R. F. Loring, D. S. Franchi, and S. Mukamel, J. Chem. Phys. **86**, 1323 (1987).
[40]D. E. Logan and P. G. Wolynes, Phys. Rev. B **31**, 2437 (1985).
[41]R. F. Loring and S. Mukamel, Phys. Rev. B **33**, 7708 (1986).
[42]R. F. Loring and S. Mukamel, J. Chem. Phys. **85**, 1950 (1986).
[43]E. Abrahams, P. W. Anderson, D. C. Licciardello, and T. V. Ramakrishnan, Phys. Rev. Lett. **42**, 673 (1979).
[44]D. Vollhardt and P. Wolfle, Phys. Rev. Lett. **48**, 649 (1982); Phys. Rev. B **22**, 4666 (1980).
[45]P. C. Martin, *Measurements and Correlation Functions* (Gordon and Breach, New York, 1968).
[46]D. Pines and P. Nozieres, *The Theory of Quantum Liquids* (Benjamin, New York, 1966).
[47]B. J. Berne and G. D. Harp, Adv. Chem. Phys. **17**, 63 (1970).
[48]D. Forster, *Hydrodynamics, Fluctuations, Broken Symmetry, and Correlation Functions* (Benjamin, New York, 1975).
[49]S. Mukamel, in *Random Walks and Their Applications in the Physical and Biological Sciences*, edited by M. F. Shlesinger and B. J. West (AIP, New York, 1984), p. 205.
[50]T. Odagaki and M. Lax, Phys. Rev. B **25**, 2307 (1982); **28**, 6480 (1983).
[51]T. G. Castner, Phys. Rev. B **21**, 3523 (1980); C. J. F. Böttcher and P. Bordewijk, *Theory of Electric Polarization* (Elsevier, Amsterdam, 1978).
[52]S. N. Dixit, P. Zoller, and P. Lambropoulos, Phys. Rev. A **21**, 1289 (1980); P. Zoller, G. Alber, and R. Salvador, Phys. Rev. A **24**, 398 (1981); H. Risken, *The Fokker–Planck Equation* (Springer, Berlin, 1984).
[53]H. Tsunetsugu, T. Taniguchi, and E. Hanamura, Solid State Commun. **52**, 663 (1984).
[54]G. S. Joyce, Philos. Trans. R. Soc. London, Ser. A **273**, 583 (1973).
[55]G. H. Hardy, *Divergent Series* (Oxford University, Oxford, 1949).
[56]G. H. Weiss and R. J. Rubin, Adv. Chem. Phys. **52**, 363 (1983).
[57]S. Chakravarty and A. Schmid, Phys. Rep. **140**, 193 (1986).
[58]Y. Gefen, A. Aharony, and S. Alexander, Phys. Rev. Lett. **50**, 77 (1983).
[59]M. Abramowitz and I. A. Stegun, *Handbook of Mathematical Functions* (National Bureau of Standards, Washington, D.C., 1972), p. 295.
[60]M. Fixman, Phys. Rev. Lett. **52**, 791 (1984).
[61]S. Havlin, M. Dishon, J. Kiefer, and G. H. Weiss, Phys. Rev. Lett. **53**, 407 (1984).
[62]H. Stehfest, Commun. ACM **13**, 47 (1970); **13**, 624 (1970).